
Since January 2020 Elsevier has created a COVID-19 resource centre with free information in English and Mandarin on the novel coronavirus COVID-19. The COVID-19 resource centre is hosted on Elsevier Connect, the company's public news and information website.

Environmental Pollution 266 (2020) 115368

Contents lists available at ScienceDirect

Environmental Pollution

journal homepage: www.elsevier.com/locate/envpol

# Diurnal and temporal changes in air pollution during COVID-19 strict lockdown over different regions of India☆

Vikas Singh [a, *], Shweta Singh [a], Akash Biswal [a, b], Amit P. Kesarkar [a], Suman Mor [b], Khaiwal Ravindra [c]

[a] National Atmospheric Research Laboratory, Gadanki, AP, India
[b] Department of Environment Studies, Panjab University, Chandigarh, 160014, India
[c] Department of Community Medicine and School of Public Health, Post Graduate Institute of Medical Education and Research (PGIMER), Chandigarh, 160012, India

ARTICLE INFO

*Article history:*
Received 15 May 2020
Received in revised form
10 July 2020
Accepted 2 August 2020
Available online 13 August 2020

*Keywords:*
Air quality
Pollution reduction
Ozone
Particulate matter
Delhi
Traffic emissions

ABSTRACT

Lockdown measures to contain COVID-19 pandemic has resulted in a considerable change in air pollution worldwide. We estimate the temporal and diurnal changes of the six criteria air pollutants, including particulate matter ($PM_{2.5}$ and $PM_{10}$) and gaseous pollutants ($NO_2$, $O_3$, CO, and $SO_2$) during lockdown (25$^{th}$ March – 3$^{rd}$ May 2020) across regions of India using the observations from 134 real-time monitoring sites of Central Pollution Control Board (CPCB). Significant reduction in $PM_{2.5}$, $PM_{10}$, $NO_2$, and CO has been found in all the regions during the lockdown. $SO_2$ showed mixed behavior, with a slight increase at some sites but a comparatively significant decrease at other locations. $O_3$ also showed a mixed variation with a mild increase in IGP and a decrease in the South. The absolute decrease in $PM_{2.5}$, $PM_{10}$, and $NO_2$ was observed during peak morning traffic hours (08–10 Hrs) and late evening (20–24 Hrs), but the percentage reduction is almost constant throughout the day. A significant decrease in day-time $O_3$ has been found over Indo Gangetic plain (IGP) and central India, whereas night-time $O_3$ has increased over IGP due to less $O_3$ loss. The most significant reduction (~40–60%) was found in $PM_{2.5}$ and $PM_{10}$. The highest decrease in PM was found for the north-west and IGP followed by South and central regions. A considerable reduction (~30–70%) in $NO_2$ was found except for a few sites in the central region. A similar pattern was observed for CO having a ~20–40% reduction. The reduction observed for $PM_{2.5}$, $PM_{10}$, $NO_2$, and enhancement in $O_3$ was proportional to the population density. Delhi's air quality has improved with a significant reduction in primary pollutants, however, an increase in $O_3$ was observed. The changes reported during the lockdown are combined effect of changes in the emissions, meteorology, and atmospheric chemistry that requires detailed investigations.



## 1. Introduction

Exposure to air pollution is one of the leading risk factors worldwide (Forouzanfar et al., 2016) as well as in India (WHO, 2018). The pollution levels in India have been reported to exceed the national ambient air quality standards (NAAQS, CPCB, 2009) (Pant et al., 2019; Singh et al., 2020a; Hama et al., 2020) and did not reduce despite measures (Gurjar et al., 2016, Chowdhury et al., 2017; Pant et al., 2019). The primary anthropogenic emission sources of particulate matter ($PM_{10}$ and $PM_{2.5}$) are households, industries, and transport sectors (Gurjar et al., 2016). In gaseous pollutants, NOx emissions are dominated by transport, industries, and coal-based thermal power plants; CO emission is due to the incomplete combustion of fuels occurring in residential biomass burning, transport sector, and industries. $SO_2$ emission is linked with the sulfur contained fuel used in different industries, coal-based thermal power plants (Sharma and Dikshit, 2016). The local anthropogenic sources are similar in different Indian regions however the total emission is proportional to the population of that region. The densely populated region of Indo Gangetic plain (IGP) has highest emissions but also impacted by regional sources such as biomass burning (Sahu et al., 2015, Beig et al., 2020; Ravindra et al., 2019a,b,c; ) and long-range transport of dust (Kumar et al., 2018). To

☆ This paper has been recommended for acceptance by Da Chen.

* Corresponding author.
*E-mail address:* vikas@narl.gov.in (V. Singh).

https://doi.org/10.1016/j.envpol.2020.115368
0269-7491/

reduce the air pollution levels, mitigation strategies and public awareness activities were launched under the National Clean Air Program (NCAP, MoEFCC, 2019) with a focus on a 20–30% reduction in PM by 2024 in India. However, the efficacy of the mitigation strategies will be known in the near future.

The implementation of nationwide lockdown due to COVID-19 (SARS-CoV-2) pandemic has resulted in a considerable change in air pollution worldwide. COVID-19 is an infectious disease that spreads primarily from humans to humans. COVID-19 was first identified in Wuhan, China and is now a pandemic affecting many countries globally. As of July 1, 2020, there have been over 10 million confirmed cases and over 500 k deaths globally (covid19.who.int). The first case in India was reported on January 30, 2020 and till July 1, 2020, there have been over 220 k active cases, 347 k cured cases and 17 k deaths (mohfw.gov.in). To prevent the spread of COVID-19, a nationwide lockdown was implemented in various phases restricting the transport and non-essential activities (MHA, 2020). The first phase was officially announced on March 24, 2020 and implemented for 21 days from 25$^{th}$ March to 14$^{th}$ April, 2020. This was extended from 15$^{th}$ April to 3$^{rd}$ May 2020 and further extended with relaxations. Before the first lockdown, day-time (07:00–21:00 h) voluntary public curfew was encouraged on March 22, 2020, followed by restrictions in affected areas. The list of activities including the transport, offices, industries restricted and permitted are listed in Supplementary Table S1. As all the non-essential services and offices were closed and the movement of the people was restricted, this has resulted in a reduction in the anthropogenic emissions. The change in the fuel consumption data (PPAC, 2020) during the lockdown suggests around 50–60%, 90%, 40%, 70% reduction in transport, aviation, industrial and construction activities respectively; and around 12% increase in household fuel consumption. Further, this has allowed researchers and policy-makers to study the impact of reduced emissions on air quality over India.

Recent studies over different countries/cities across the Globe (Mausam and Pal, 2020; Nakada and Urban, 2020; Krecl et al., 2020; Dantas et al., 2020; Bao and Zhang, 2020; Li et al., 2020; Wang et al., 2020a, 2020b; Huang et al., 2020; Zheng et al., 2020; Fan et al., 2020; Sicard et al., 2020; Jain and Sharma, 2020; Mandal and Pal, 2020; Mahato et al., 2020; Sharma et al., 2020; Srivastava et al., 2020; Sarfraz et al., 2020; Navinya et al., 2020; Selvam et al., 2020; Kumari and Toshniwal, 2020; Fattorini and Regoli, 2020; Collivignarelli et al., 2020; Kerimray et al., 2020; Abdullah et al., 2020; Otmani et al., 2020; Tobias et al., 2020; Menut et al., 2020; Kanniah et al., 2020; Bashir et al., 2020; Lal et al., 2020; Chauhan and Singh, 2020; Zambrano-Monserrate et al., 2020; Muhammad et al., 2020) have found changes, mainly a decline in $PM_{2.5}$, $PM_{10}$, $NO_2$ and CO and enhancement in $O_3$. Kindly refer to Supplementary Table S2 for details. It is estimated that excessive risk and mortalities associated with air pollution might have reduced during lockdown (Yongjian et al., 2020; Dutheil et al., 2020; Chen et al., 2020; Isaifan, 2020; Filippini et al., 2020; Sharma et al., 2020).

Studies over Indian cities and regions have reported significant improvement in air quality (Sharma et al., 2020; Mahato et al., 2020; Jain and Sharma, 2020; Srivastava et al., 2020; Sarfraz et al., 2020; Navinya et al., 2020; Kumari and Toshniwal, 2020; Selvam et al., 2020; Mandal and Pal, 2020) during the lockdown. A significant reduction in $NO_2$ has been observed from space (ESA, 2020). Mahato et al. (2020) has analysed the CPCB real-time air quality data at 34 monitoring stations in Delhi for the period of 3$^{rd}$ March to 14$^{th}$ April 2020 and reported a significant reduction in $PM_{10}$, $PM_{2.5}$, $NO_2$ and CO and 40–50% improvement in the national air quality index during the lockdown. The study by Sharma et al. (2020) reported around 43, 31, 10, and 18% decrease in $PM_{2.5}$, $PM_{10}$, CO, and $NO_2$ respectively using CPCB real-time air quality data at 22 locations in different regions of India. However, the study period was for a shorter period, i.e., starting from 16$^{th}$ March to 14$^{th}$ April 2020, which does not coincide with the actual lockdown period. Jain and Sharma (2020) considered even shorter period (25$^{th}$ March to 6$^{th}$ April 2020) to study the change over five megacities of India and reported that $PM_{2.5}$, $PM_{10}$, $NO_2$ and CO were declined by ~41%, ~52%, ~51%, and ~28% respectively during the lockdown as compared to before lockdown in 2020 in Delhi as well as a similar decline in other megacities. It is known that primary emitted pollutants are likely to decline during winter-spring-summer because of the favourable meteorological conditions. Therefore, estimating decline with respect to before lockdown in the same year may also include the seasonal decline in the pollution levels. Sarfraz et al. (2020) have analysed the reduction over two cities (Mumbai and Delhi) using the CPCB and Sentinel-5P satellite images to show a reduction of 40–50% in $NO_2$. Srivastava et al. (2020) analysed four pollutants over Lucknow and New Delhi and found a significant decline. Kumari and Toshniwal (2020) have shown a lesser reduction in smaller cities than metro cities. Selvam et al. (2020) have focussed their study on Gujarat region whereas Mandal and Pal (2020) have shown a reduction near the stone crushing site. Navinya et al. (2020) noticed a reduction in $PM_{2.5}$, $PM_{10}$, $NO_2$, and CO over 17 cities in India during the lockdown period. They also analysed hourly data averaged over all 17 sites and found maximum reduction during the morning (7–10 a.m.) and evening (7–10 p.m.) periods. While studies by Mahato et al. (2020); Jain and Sharma (2020); Kumari and Toshniwal (2020) and Srivastava et al. (2020) have focussed only over the cities, Sharma et al. (2020) reported the changes over different regions but with limited sites not coinciding the actual lockdown period. Most importantly, all the studies considered data less than three weeks which may have been influenced by the synoptic meteorology which has a variability of few weeks (Seo et al., 2018; Hogrefe et al., 2003; Eskridge et al., 1997). As the short-term (micro, meso- and synoptic-scale) meteorological variation can improve/deteriorate the air quality for a short period despite emission reduction during lockdown (Wang et al., 2020b; GLA, 2020), an extended period greater than the time scale of the meteorology can minimize the impact of short-term changes in the meteorology. Although Navinya et al. (2020) have used the data of six weeks, however, their study was limited to 17 sites. They reported the changes in diurnal variation averaged across 17 locations that may not represent the spatial variability of pollution across different regions of India (Guttikunda et al., 2019; Purohit et al., 2019; WHO, 2018). Moreover, they did not include $O_3$ in their study, which is one of the critical pollutants. Further, their analysis was limited to 2019 and 2020. The current study examines the available ground-based (134 sites) six criteria air pollutants ($PM_{2.5}$, $PM_{10}$, $SO_2$, $NO_2$, $O_3$, and CO) obtained from the Continuous Ambient Air Quality Monitoring Stations (CAAQMS) of Central Pollution Control Board (CPCB), Delhi over different geographical regions of India. The study aims to estimate the changes in air pollution during the strict phases of lockdown (25$^{th}$ March – 3$^{rd}$ May 2020) by conducting extensive analysis in terms of daily variation, diurnal variation as well as overall changes over different geographical regions of India.

## 2. Data and method

### 2.1. CPCB data

The hourly averaged data of $PM_{2.5}$, $PM_{10}$, $NO_2$, $O_3$, CO and $SO_2$ at 134 sites (supplementary Figure S1; Table S3) from 15$^{th}$ February to 3$^{rd}$ May each year for four years from 2017 to 2020 was acquired from CAAQMS situated across India (https://app.cpcbccr.com/ccr/#/caaqm-dashboard-all/caaqm-landing), which is managed by

CPCB, Delhi. The methodology used for measurement of each pollutant is shown in the Supplementary Table S4 and technical details can be found in CPCB (2019). The sites have been grouped according to the six geographical regions (north, IGP, north-west, north-east, central and South) based on their pollution status and sources; and for the better presentation of the results. The map of the different regions and the location of the sites is shown in Figure S1. The states under different zones are tabulated in Supplementary Table S3. The IGP region covers from Punjab to West Bengal, having the highest population density and is one of the most polluted regions (Guttikunda et al., 2019; Purohit et al., 2019; WHO, 2018). Gujarat and Rajasthan, under the north-west region, are often under the influence of dust-storms originating locally and sometimes across the middle east region (Yadav et al., 2017). The Central zones stretched from Maharashtra to Odisha, and the states on the southern peninsular region of India were chosen as the south region. North and north-east regions have not been considered because of a less number of sites.

The quality of data was ensured by filtering the outliers and constant values. The data, which is more than three local scaled Median Absolute Deviations (MAD) from the local median of the data within a running window of 24 h, was considered as an outlier. The concentrations at a site having a standard deviation of less than 5% of the mean were recorded as having erroneous constant data, and therefore are not considered. Missing records, erroneous data and outliers in the observation have not been considered for the analysis considering them as invalid data. Sites having more than 60% of valid data during the analysis period were considered in the study. This data quality check resulted in 134 valid sites for the analysis. As the measurement status differs according to site and pollutant, the number of valid sites for $PM_{2.5}$, $PM_{10}$, $NO_2$, $O_3$, CO and $SO_2$ are 121, 100, 100, 93, 96 and 90 respectively. The number of sites in each region is shown in Supplementary Table S5.

Additionally, we use the time-averaged Modern-Era Retrospective Analysis for Research and Applications, version 2 (MERRA-2) reanalysis monthly meteorological products during lockdown months from 2017 to 2020 to compare the metrology during the lockdown with the previous year of meteorology. The MERRA-2 data was obtained from NASA's Global Modeling and Assimilation Office (GMAO) at a horizontal resolution of $0.5^\circ \times 0.625^\circ$ (https://gmao.gsfc.nasa.gov/reanalysis/MERRA-2/). Details of the MERRA-2 products and evaluation has been reported by Gelaro et al. (2017), Randles et al. (2017) and Buchard et al. (2017).

### 2.2. Data analysis

Hourly data from 15$^{th}$ February to 3$^{rd}$ May for four years from 2017 to 2020 have been analysed to study the temporal variation of the pollutants during the transition from the before lockdown to lockdown. Further, the changes in the pollutants were estimated during the lockdown period (25$^{th}$ March to 3$^{rd}$ May 2020) and compared with the same period during the previous years.

The meteorology during the lockdown period was observed to be similar during 2017–2020 (Section 3.1). The data set has been divided into reference year (2017–2019), and the current year (2020) for comparison. The percentage change has been calculated using the following equation

$$D = \frac{Yc - Yr}{Yr} \times 100$$

where.

D is the percentage change, Yc is the average concentration of a pollutant in the current year during the lockdown period, Yr is the average concentration of a pollutant in reference years during the lockdown period.

Changes in the pollutants have been reported for each region in terms of the mean, median and IQR of the changes estimated for all sites within a region.

## 3. Results

### 3.1. Meteorology and air mass trajectories over India during lockdown

The changes in pollutants level during the COVID-19 lockdown across India can partially or significantly be affected by the meteorological conditions during this period. However, changes in the air pollution due to the emission change can be studied by comparing the average pollutant concentrations under the same meteorological conditions (Li et al., 2019; Cheng et al., 2017). We compare the MERRA-2 meteorological parameters during 2017–2019 with the 2020 during lockdown months (March–May). Time-averaged 10-m wind speed and direction, 2-m temperature and precipitation are shown in Supplementary Figure S2. The 10-m wind speeds show anticyclonic motion over the Bay of Bengal and the Arabian Sea shows similar spatial variations in wind pattern. The prevailing of north westerlies from NW India to Central India and interior south Indian regions can be seen from the figure. The warm air cause increase in surface temperatures seen over Central India and interior south Indian regions. Wind discontinuity also can be seen in the 10-m plots. The average rainfall over India varied from 0 to 2.5 mm/day during this period. The enhancement in precipitation due to Norwesters can be seen over Bangladesh and Northeast Indian region in both the plots. In general, all the meteorological parameters follow a similar spatial variation. The similarity in the meteorological parameters is confirmed by recent studies. Sharma et al. (2020) have reported similar meteorology over the years 2017–2019 and 2020 during the one-month analysis period around the lockdown. Moreover, Navinya et al. (2020) have also reported that the daily variations in wind speed, temperature, and relative humidity averaged over 17 cities show similar variations during the same period in 2019 and 2020. Additionally, we performed the five days backward trajectories analysis using the Hybrid Single Particle Lagrangian Integrated Trajectory (HYSPLIT) model (Stein et al., 2015) to characterize air masses. Five days backward trajectories arriving at 500 m were computed at an interval of 6 h. Then, cluster analysis was carried out to identify five major trajectories during the lockdown as shown in Supplementary Figure S3. For northern India, the majority of the air masses originate from inland as well as from the transboundary region in the west. The most densely populated IGP region receives most of the air masses from within IGP as well as transboundary regions. North eastern region receives air masses from nearby regions. During this season, the majority of air masses for central, western, and southern parts of India originate from the oceanic region, with the Arabian sea for the western region and the Arabian sea along with Bay of Bengal for central India and southern Indian region. The HYSPLIT trajectory plot directions are similar to the wind vectors shown in Figure Supplementary Figure S2.

### 3.2. Temporal evolution of the pollutants before and during lockdown periods

Air pollutants are known to vary diurnally, monthly, seasonally and inter-annually in different environments (Pant et al., 2019; Singh et al., 2020a; Masiol et al., 2017; Singh et al., 2018a; Im et al., 2015a, 2015b; Xing et al., 2015). The local meteorology and emissions govern the variations at a given geographic location. Primary emitted pollutants are likely to decrease during winter to spring

because of the change in meteorological conditions (increased planetary boundary layer height, PBLH), whereas $O_3$ increases from winter-spring-summer transition because of the photochemical production. However, some pollutants show a peak in different months due to forest fires, biomass burning (Yin et al., 2019) or agricultural activities (Tang et al., 2018).

A comparison of pollutants with the pre-lockdown period may include the seasonal component. Therefore, it would be appropriate to compare the trend in the pollutants concerning the previous years as reference years.

### 3.2.1. $PM_{2.5}$ variation

Variations in $PM_{2.5}$ are shown in Fig. 1. In general, a decreasing trend in $PM_{2.5}$ can be observed across all regions because of the winter-spring-summer transition (Singh et al., 2020a). IGP region was identified as most polluted, where the levels of $PM_{2.5}$ varies between ~50 and 100 μg/m$^3$. $PM_{2.5}$ was found in the range of 30–60 μg/m$^3$, ~40–80 μg/m$^3$, and ~30–50 μg/m$^3$ in central India, north-west and south India respectively. The values for North-west and IGP region were of most fluctuating nature with the association of dust storm in the western part of India (Yadav et al., 2017), biomass burning (Sahu et al., 2015), and higher winds associated with summer season (Kumar et al., 2018) in IGP region. During the lockdown period, $PM_{2.5}$ decreased significantly for all the regions having similar variabilities, as seen in the previous years. $PM_{2.5}$ decreased quickly just after the lockdown, then increased around 10$^{th}$ April and later decreased. The ratio of $PM_{10}$ and $PM_{2.5}$ suggests that the increasing spell of $PM_{2.5}$ could be associated with a dust storm. It can be seen in Fig. 1 that IGP continued to be the most polluted, and the South remained the cleanest during the lockdown. Moreover, the average pollution during the first and second lockdown follows a similar pattern for $PM_{2.5}$ across all the regions. Faster drop just after the lockdown over IGP, North-West, and Central, was observed (Fig. 1). Mahato et al. (2020) have made similar observations; however, it has to be noted that emission reductions solely could not be attributed to lockdown but also could be due to the western disturbances (WDs, Dimri et al., 2015). WDs play a critical role in the meteorology of the Indian subcontinent during November to March. WDs are associated with higher wind speed, thunderstorms, and rainfall over northern and north-west parts of India including the IGP.

### 3.2.2. $PM_{10}$ variation

The variations in the daily mean $PM_{10}$ are shown in Supplementary Figure S4. A decreasing trend in $PM_{10}$ was observed over the central and south India in the previous years, except for IGP and the north-west region. This could be due to the long-range transport of dust from the desert (Kumar et al., 2018) that affects the $PM_{10}$ levels in the North-west and IGP regions during summer months. For $PM_{10}$ also, as observed for $PM_{2.5}$, the highest concentration was observed in the IGP region with maximum fluctuations.

During the lockdown period, $PM_{10}$ showed a significant decline for all the regions, having the highest reduction in the IGP region. The reduced vehicular movement, limited industrial and construction activities can be responsible for the decline in $PM_{10}$ emissions. The restricted movement of vehicles can also be a means of reduction of the exhaust (Singh et al., 2018b), and non-exhaust emissions (Singh et al., 2020b), mainly resuspended dust, in the coarse part of PM. A large difference can be observed across the air pollution monitoring sites in the IGP and north-west region, where surface dust load is relatively high in the PM (Parajuli and Zender, 2017). The $PM_{10}$ concentration, which was found to be in the range of ~80–270 μg/m$^3$ in IGP and 90–140 μg/m$^3$ in the central and north-west regions in the previous years has been reduced to ~70 μg/m$^3$ during the lockdown. A significant reduction is also seen in the South region.

### 3.2.3. $O_3$ variation

$O_3$ is a secondary pollutant that is formed in the presence of sunlight and its precursors viz, nitrogen oxides (NOx), and volatile organic compounds (VOCs). Its concentration varies according to photochemistry, physical/chemical removal, and transport over local, regional, and global scales (Lal et al., 2000; Reddy et al., 2012). $O_3$ shows an almost constant trend with some fluctuations for all

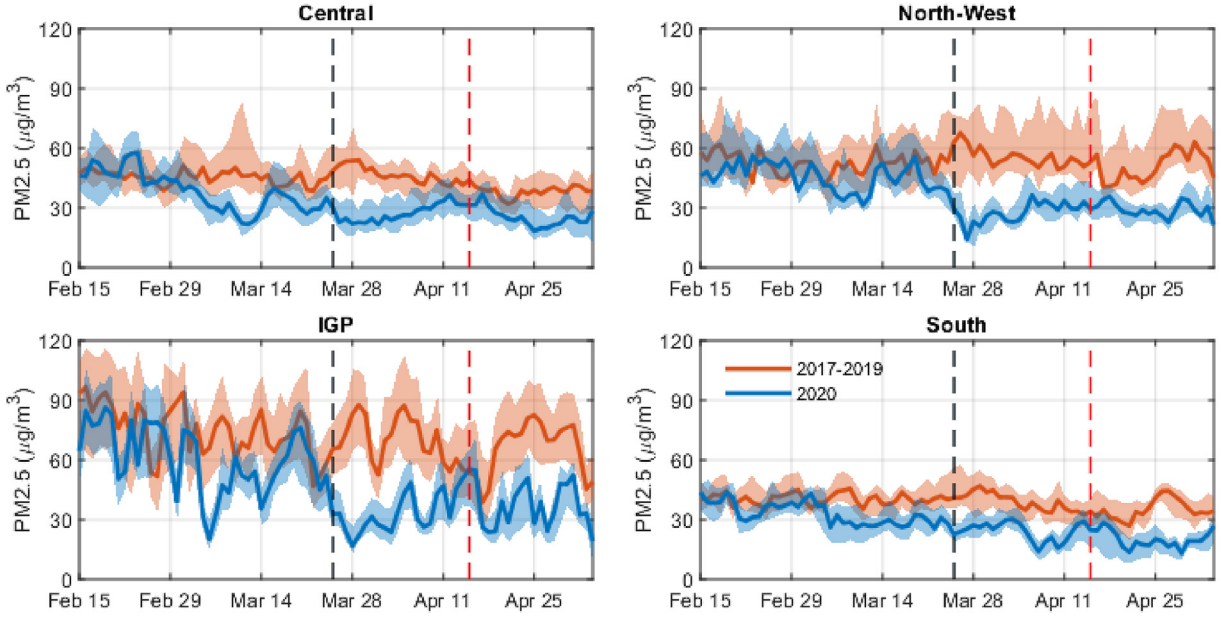


**Fig. 1.** Temporal evolution of daily mean $PM_{2.5}$ concentration before and during the lockdown period for the four study regions. The line plot shows the median and shaded region shows the IQR of mean levels observed at the sites in the respective regions. Vertical black and red lines mark the beginning of 1st and 2nd phases of lockdown respectively. (For interpretation of the references to colour in this figure legend, the reader is referred to the Web version of this article.)

the regions except for the sites in the IGP (Fig. 2), where it shows a continuously increasing trend amid the increase in solar radiation. Additionally, biogenic emissions of isoprenes, a precursor for $O_3$ formation, and biomass burning related $O_3$ production, help in the rise of $O_3$ concentration during the summer season. It has been previously reported that among all the regions of India, biomass burning associated $O_3$ production was observed to be highest over central India (Lu et al., 2018).

During the lockdown period, a decline in $O_3$ concentration was observed at the sites in south India, and for a few days over central India and a slight increase over the IGP. However, a decrease in the $O_3$ concentration in 2020 in the South was also observed before the lockdown that requires further investigation. The reduction of $O_3$ over the southern part can be attributed to the decrease in the $O_3$ precursors in the northern region, which is horizontally transported to the South (Kumar et al., 2012; Lu et al., 2018) in this season. Moreover, the rise in the humidity and temperature over the southern region may have led to the reduction of $O_3$ as it reacts with water vapor to form OH radicals in the atmosphere. For the North-west region, the concentration during and before lockdown remained almost similar having a fluctuating trend.

### 3.2.4. $NO_2$ variation

$NO_2$ variation before and during the lockdown is depicted in Fig. 3. $NO_2$ is emitted from biogenic sources like soils and lightning, pyrogenic sources like natural fires, and anthropogenic sources like vehicular emission and fossil fuel-based power plants (Reddy et al., 2012). $NO_2$ controls the formation of $O_3$. In the previous years, $NO_2$ shows a slightly decreasing trend for all the regions except the IGP, where it shows an almost constant trend. The decrease could be due to the seasonal transition to summer, as the gaseous pollutant is found to be highest during the winter season (Ghosh et al., 2017). During the lockdown period, all the regions showed a marked decline in concentration with the highest level observed across the IGP and north-west region. This decrease in $NO_2$ could be mainly attributed to reduced vehicular emissions. The reduction in $NO_2$ in the IGP region during the lockdown was also reported by Sharma et al. (2020) and Mahato et al. (2020).

### 3.2.5. CO variation

Variations of carbon monoxide (CO) are shown in Supplementary Figure S5. CO is mostly emitted from vehicular sources. However, other sources include forest fires, agricultural waste burning, biofuel burning, and oxidation of hydrocarbons and combustion of fossil fuels (Holloway et al., 2000). The higher concentration of CO is observed at the sites in the central and IGP region during the previous three years (~800–1000 μg/m$^3$). In the Central region, some sites observed concentrations up to 1500 μg/m$^3$. Higher levels can be attributed to biofuel usage in densely populated IGP, whereas the levels in central India could be due to forest fires and agriculture burning, predominant during this season as observed by Sahu et al. (2015). The concentration of CO declined for all the four regions during the lockdown, and this is mainly due to restriction in vehicle movement. As CO has a relatively long lifetime, it can be transported over a longer distance. The levels of CO at the sites in all the regions were found to be around 500 μg/m$^3$ during the lockdown.

### 3.2.6. $SO_2$ variation

The primary source of $SO_2$ is the combustion of sulfur-containing fuels, i.e., coal and diesel used in thermal power plants, industries, and transport (Lu et al., 2013; Gaur et al., 2014). $SO_2$ can also be sourced from volcanic eruptions (Mallik and Lal, 2014) and wildfires. For the Indian scenario, the primary anthropogenic source of $SO_2$ is coal-fired thermal power plants as reported by (Lu et al., 2013; Mallik and Lal, 2014). Six states UP, Gujarat, Maharashtra, Chattisgarh, Odisha, and Tamil Nadu, accounted for 60% of the total emission of $SO_2$ in the year 2012 (Lu et al., 2013). Variation in $SO_2$ before and during the lockdown period for the four regions of India are shown in Supplementary Figure S6. The median value of $SO_2$ in the previous years was recorded highest for the IGP (~10–15 μg/m$^3$) region followed by North-west and Central India. Unlike $O_3$ and particulate matter, the levels of $SO_2$ remained the same for the considered period for all the areas in the previous years. This year, $SO_2$ levels show a small decline during lockdown for all the regions except for South India.

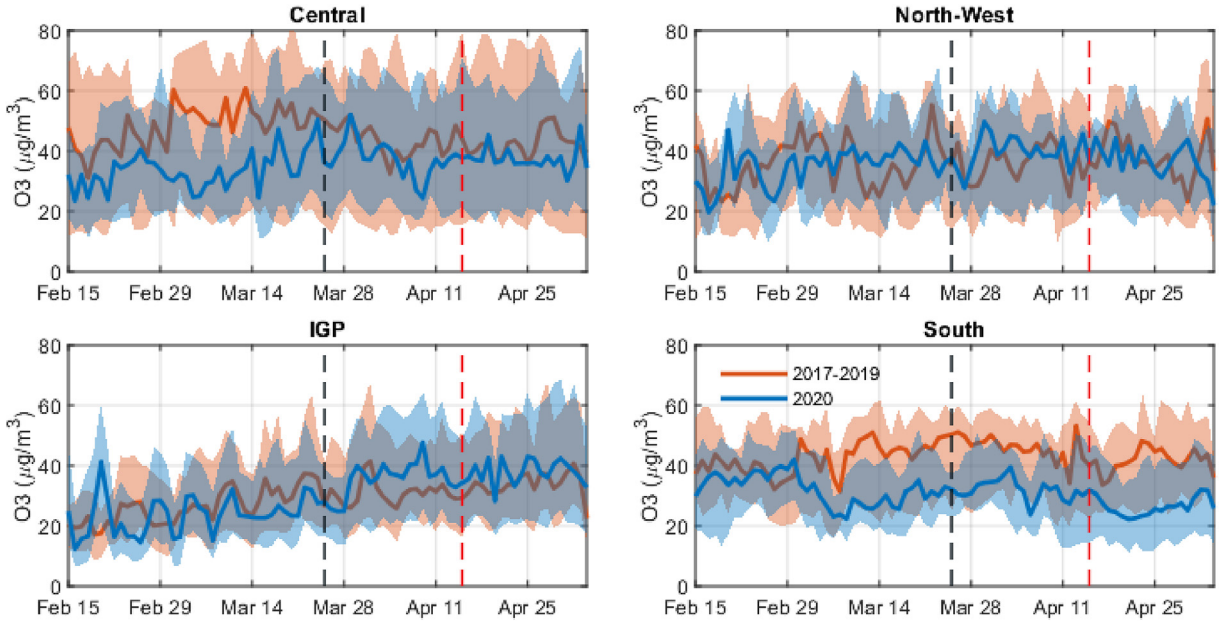


**Fig. 2.** Temporal evolution of daily mean $O_3$ concentration before and during the lockdown period for the four study regions.

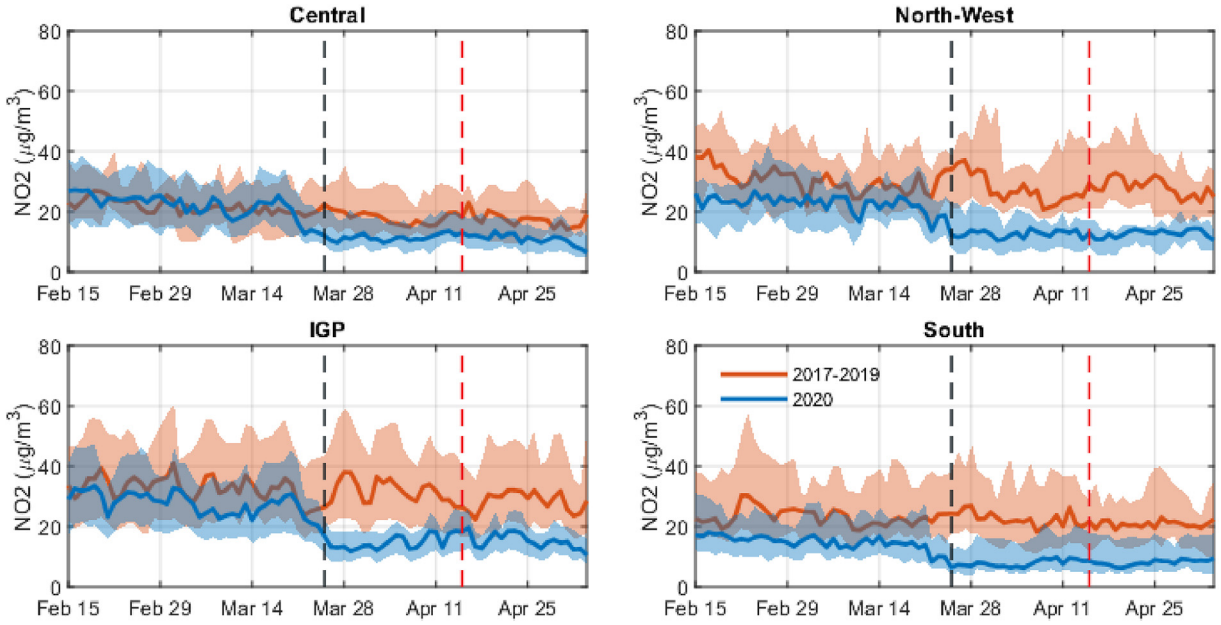


**Fig. 3.** Temporal evolution of daily mean $NO_2$ concentration before and during the lockdown period for the four study regions.

### 3.3. Changes in the diurnal variations of the pollutants

In this section, we investigate the changes in the diurnal variation in the pollutant during the lockdown. Diurnal variation of a pollutant is mainly governed by the local emissions, meteorological condition, and; day-time and night-time chemistry. However, the relation between pollutant concentration and controlling factors is non-linear because of the complex chemistry and atmospheric dynamics (Seinfeld and Pandis, 2006). The reduction in the primary anthropogenic emissions can lead to changes in the pollutant concentration at a different hour of the day. Therefore, we compare the diurnal variation (00–23 h) of all six pollutants this year (2020) with reference to the average diurnal variation observed in the previous years (2017–2019) and shown in Fig. 4. Additionally, absolute change (Fig. 5) and percentage change (supplementary Figure S7) at a different hour of the day have also been shown and discussed.

#### 3.3.1. Diurnal variation of particulate matter ($PM_{2.5}$ and $PM_{10}$)

The normal diurnal variation of $PM_{2.5}$ and $PM_{10}$ (Fig. 4) shows a bimodal distribution with two peaks observed in the morning and evening at the sites in all the regions. The morning peak (~0800–1000 h) is due to the fumigation effect and traffic emissions whereas the evening and the nigh-time increase is associated with the household emission (Yadav et al., 2017; Ravindra et al., 2019a, 2020; Kaur-Sidhu et al., 2020; Singh et al., 2020a) and lower dispersion due to reduced planetary boundary layer height (Schnell et al., 2018). The lowest level of PM was observed during the late afternoon hours (~15:00–16:00 h) in all regions. However, monitoring sites in the south show minimum value after midnight.

The diurnal variation in $PM_{2.5}$ and $PM_{10}$ during the lockdown shows a significant reduction throughout the days, and the variability remains the same. All the locations continue to have morning and evening peaks, as observed in the previous years. The peak concentration of $PM_{2.5}$ and $PM_{10}$ were observed in the IGP, which were in the range of 70–110 μg/m$^3$ and 150–280 μg/m$^3$ respectively during previous years, were reduced by 50–60% to the level of 35–50 μg/m$^3$ and 70–120 μg/m$^3$, respectively during the lockdown. While the percentage reduction of 40–50% in PM is constant throughout the day (Supplementary Figure S7), the absolute reduction varies according to the time of the day (Fig. 5). The maximum reduction has been found during the night-time as well as during the peak traffic hours, whereas the absolute minimum reduction was found during the afternoon hours. In general, the $PM_{10}$ level has been reduced by 70–140 μg/m$^3$, 40–90 μg/m$^3$, 40–70 μg/m$^3$ and 30–50 μg/m$^3$ at the sites in IGP, north-west, central and south regions respectively. Similarly, $PM_{2.5}$ concentration reduced by ~40–60% across all the regions (supplementary Figure S7). The reduction during peak traffic hours can be explained by the decrease in traffic emissions. Assuming that the household emissions have either not changed or increased marginally, and the emission from coal-based tandoors in restaurants/hotels and street food (Sharma and Dikshit, 2016) have reduced, the reduction in the night time is more than expected therefore requires detailed investigation.

#### 3.3.2. Diurnal variation of $O_3$ and $NO_2$

$NO_2$ is the major precursor of tropospheric and surface $O_3$; therefore, the diurnal variation of $O_3$ depends on $NO_2$. As the atmosphere of most of the cities of north, west, and south India is VOC limited (Sharma et al., 2016; Kumar et al., 2008), the diurnal trend of $O_3$ will closely follow a negative correlation with that of its major precursor $NO_2$. In previous years, the diurnal variation of the $NO_2$ involves an increasing level till morning 08:00–09:00, then it starts to decrease, before again rising during the night-time. After the morning peak, $NO_2$ gets involved in a photo-dissociation cycle where the formation and destruction of $O_3$ molecules take place. However, the diurnal variation of $O_3$ during the typical day does not precisely complement that of $NO_2$, therefore it confirms the involvement of other precursors like VOCs and CO and $CH_4$. The traffic associated morning $NO_2$ peak can be observed across all the regions. Moreover, night-time $NO_2$ was found to be more than the day-time peak. The enhancement in the day-time peak was restricted by the photochemical production of $O_3$ (Seinfeld and Pandis, 2006). The maximum concentration of $O_3$ was observed in the late afternoon hours for all the regions with the maximum value obtained for the IGP and north-west region (~70–90 μg/m$^3$). The minimum $O_3$ concentration was found in the morning hours

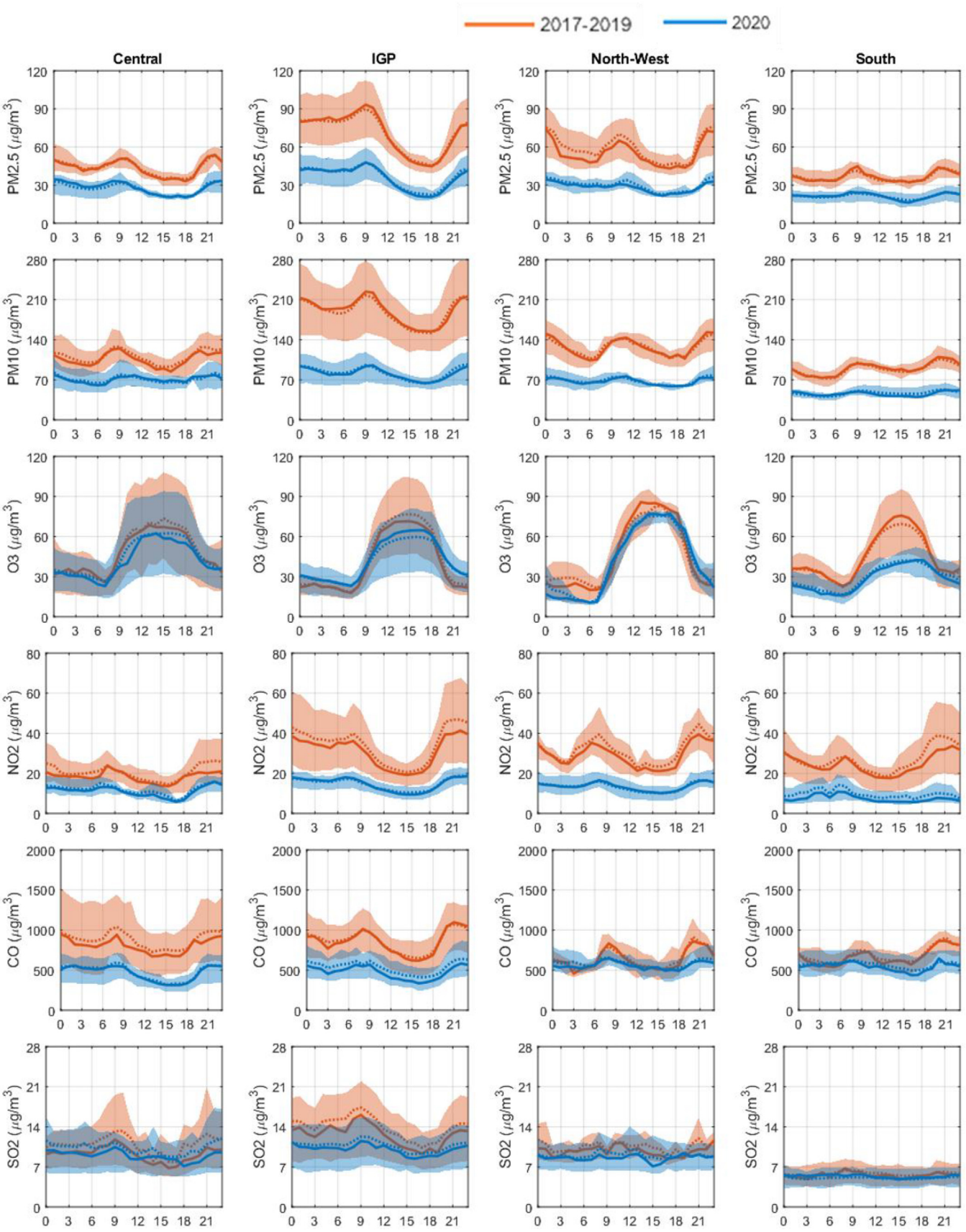


**Fig. 4.** Diurnal variation of the six criteria pollutants before and during the lockdown period for the four study regions. The red plot shows the diurnal variation in the pollutants in the previous years and the blue plot is for the current year. Continuous line and the dotted line represent the median and mean respectively and the shaded region shows the IQR of

(6–7 am) for all the regions.

During the lockdown, diurnal variation follows a similar trend for both $NO_2$ and $O_3$ across all regions. However, the reduction in $NO_2$ was found throughout the day, whereas the decrease in $O_3$ is limited during the sunlight hours. The reduction in $NO_2$ levels during night hours was observed to be more than the day-time. Night-time enhancement in $O_3$ of ~20–30% or even higher is also seen in the IGP and north-west regions. Night-time enhancement in $O_3$ is because of the reduction in the removal of $O_3$ at night. While Nitrogen oxides help in the photochemical production of $O_3$ during the day, it forms nitric acid, oxidizes hydrocarbons, and remove $O_3$ at night (Brown et al., 2006).

Moreover, heterogeneous chemistry near the surface involving aerosols can also be responsible for the direct loss of $O_3$ (Jacob, 2000). This is evident from the $O_3$ diurnal variation that the night level of $O_3$ in the polluted region (i.e., IGP) in the previous years was lower than the night-time levels in a less polluted region of the South. The same can be seen in the differences in the levels of $O_3$ during the day and night, which was observed to be highest for IGP and north-west. A significant reduction in $NO_2$ and PM in the night-time can be responsible for the night-time enhancement in $O_3$. However, the enhancement is not consistent across all the sites because of the complex chemistry.

### 3.3.3. Diurnal variation of CO

CO being a biomass and traffic-related pollutant, shows a bimodal distribution during normal days for all the regions with peaks being most prominent for the North-west region. Moreover, the levels are higher in IGP and central regions owing to biomass activities (Sahu et al., 2015; Venkataraman et al., 2006). The highest concentration was observed in the IGP and central regions during night time (~1000 $\mu g/m^3$) and lowest during late afternoon hours. As CO is also a precursor for $O_3$ formation, it is utilized maximum during the afternoon for $O_3$ formation with NOx as a catalyst leading to low levels of CO during the afternoon (Lal et al., 2000). During the lockdown phase, the peaks are still visible, yet less prominent. The difference in concentration is highest for the IGP region with the maximum reduction during late-night hours (Fig. 5). While for the IGP region, the median percentage reduction is roughly similar across the day, for the North-West region, the reduction percentage is significantly lower during afternoon hours.

### 3.3.4. Diurnal variation of $SO_2$

The diurnal variation of $SO_2$ shows a prominent morning peak in IGP and central regions; and smaller peaks in other regions during the previous years. The highest concentration of $SO_2$ was observed in the IGP region, and the lowest levels were observed for south India during afternoon hours. A considerable reduction can be seen during the lockdown in the IGP region. The absolute concentration difference during lockdown was observed to be highest for the IGP (maximum during early morning hours) and least for south India (Fig. 5). For the IGP, the percentage decline during lockdown (supplementary Figure S7) was observed significant during morning hours, whereas it became negligible in the afternoon due to the increase in PBLH. In contrast to the other three regions, the percentage increase in $SO_2$ was observed for a few sites in south India. The increase over the southern region could be a result of the decrease of the $SO_2$ oxidation due to the decline of $O_3$ concentration in the presence of NaCl particles, which are abundant in the south Indian peninsula surrounded by oceans (Li et al., 2007).

### 3.4. Overall percentage reduction in regions of India

The overall decrease in the concentration of the six criteria air pollutants is shown in Fig. 6 as a box plot. The red line in the box shows the median value, and the box shows the interquartile range. The red star shows the average change. A substantial reduction can be observed for most of the pollutants. The significant decrease was identified for $PM_{2.5}$ and $PM_{10}$, where the reduction was ~50%. Although this study does not cover the north-east region and the northern part of the country, still the overall observed percentage reduction in air pollutants (averaged over the four areas) can be representative of the whole country during the lockdown period. The estimated changes in the concentrations for different regions are shown in Table S5.

In contrast to previously reported results of Sharma et al. (2020), which has reported 43% and 31% reduction in $PM_{2.5}$ and $PM_{10}$ respectively, our study found around ~40–60% reduction for both $PM_{2.5}$ and $PM_{10}$. Considering the four regions separately, the highest $PM_{2.5}$ and $PM_{10}$ reduction were observed for the North-west region (~50–60% for both $PM_{10}$ and $PM_{2.5}$), followed by the IGP region (~40–60% for both $PM_{10}$ and $PM_{2.5}$). In the case of gaseous pollutants, CO and $NO_2$ showed reductions in all four regions. $SO_2$ showed mixed variation with a decrease in the mean value in the south, IGP and north-west. Ozone was found to have mixed behavior; however, it has shown a decrease at most of the sites and a moderate increase over the IGP region. A reduction in $O_3$ was recorded in the south and central region.

Our results vary slightly from those of Sharma et al. (2020) who have reported 34% reduction in $PM_{2.5}$ and a slight increase in $SO_2$ for IGP. The current study observed a decrease in $SO_2$ and a mild increase in $O_3$ at most of the sites in the IGP, and ~60% reduction for $PM_{2.5}$ at all sites. In the case of the southern region, this work computes a $NO_2$ reduction in agreement with Sharma et al. (2020), whereas for CO our results contrast their observation and find a reduction in CO levels.

### 3.5. Change in the probability distribution of pollutants

The probability density function (PDF) using kernel density estimation (KDE) of all six pollutants during the lockdown in 2020 and during the same period in 2017–2019 for all regions have been shown in Fig. 7. KDE is a non-parametric way to estimate the PDF. The peak of the distribution shows the most probable value and the width of the distribution shows the variability. It can be seen from Fig. 7 that the variability and the most probable concentration of the $PM_{2.5}$, $PM_{10}$, $NO_2$, and CO have reduced significantly in all the regions during the lockdown. Whereas $SO_2$ shows marginal change and $O_3$ does not exhibit a significant change in the probability distribution except for the south region where it shows reduction. The most probable value of $PM_{2.5}$ has been reduced from 44 to 27 $\mu g/m^3$, 69 to 37 $\mu g/m^3$, 52 to 30 $\mu g/m^3$, and 37 to 22 $\mu g/m^3$ respectively over Central, IGP, North-West and South regions. Similarly, $PM_{10}$ has been reduced significantly in all the regions with maximum reduction in the IGP. During the lockdown, the most probable value of $PM_{10}$ was estimated to be 67 $\mu g/m^3$, 84 $\mu g/m^3$, 68 $\mu g/m^3$, and 46 $\mu g/m^3$ respectively. The most probable concentration of $NO_2$ was reduced from 18 to 11 $\mu g/m^3$, 27 to 15 $\mu g/m^3$, 25 to 13 $\mu g/m^3$, and 19 to 8 $\mu g/m^3$ over Central, IGP, North-West and South regions respectively. The reduction in most probable CO concentration was found to be highest for IGP and least for the North-west region. The most probable value of $SO_2$ has reduced

mean diurnal variation observed at the sites in the respective regions. (For interpretation of the references to colour in this figure legend, the reader is referred to the Web version of this article.)

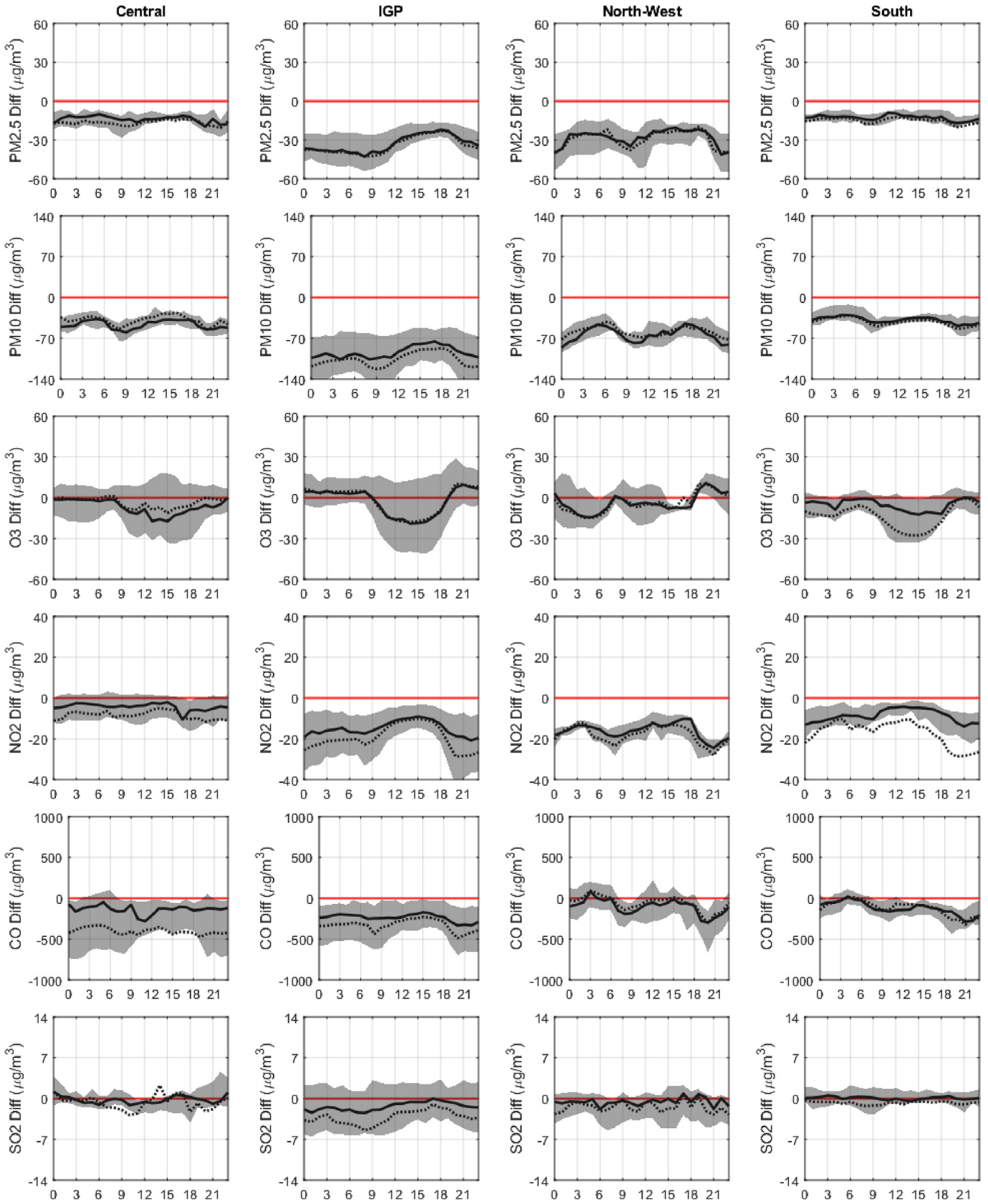


**Fig. 5.** Diurnal variation of the absolute difference in the concentration of six criteria pollutants during the lockdown period against their respective average for reference years (2017–2019). Continuous line and the dotted line represent the median and mean respectively and the shaded region shows the IQR.

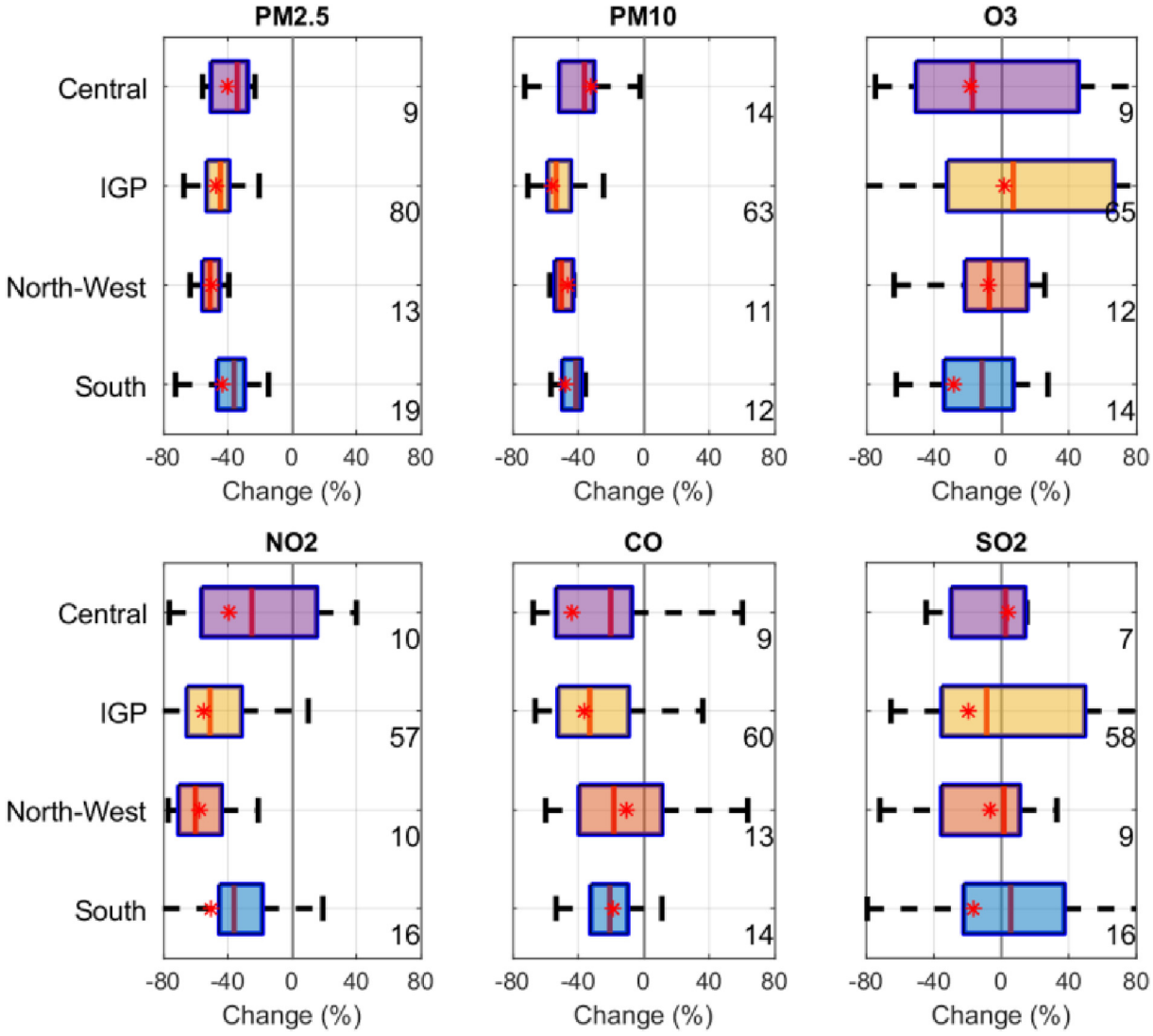


**Fig. 6.** Box plot of the percentage change in the six criteria pollutants across the four study regions during the period of two phases of lockdown. The red line in the box shows the median value, red star indicates the mean value. and the box shows the interquartile range. Numbers on the right side are the number of stations used for the box plot. (For interpretation of the references to colour in this figure legend, the reader is referred to the Web version of this article.)

marginally in all regions. The probability distribution of $O_3$ shows a decrease in higher values but a slight increase in the most probable values over Central, IGP, and north-west regions and a significant decrease in the south region. The non-linear chemistry of $O_3$ has been explained in section 3.3.2.

### 3.6. Air pollution changes with population

Pollution change has been analysed with respect to population density. Population data corresponding to the CPCB monitoring station has been taken from WorldPop (2017). Fig. 8 shows the scatter plot of the change of the six pollutant concentrations with the population/km$^2$. The least-square fit with the slope value is also shown. Fig. 8 shows a significant negative slope for $PM_{2.5}$, $PM_{10}$ and $NO_2$, a positive slope for $O_3$ and almost a very small negative slope for CO and $SO_2$. This suggests that amount of reduction in $PM_{2.5}$, $PM_{10}$ and $NO_2$ is directly proportional to population density. Similar results were observed by Wang et al. (2020a) who compared the pollution reduction with vehicle density (proportional to population density) in northern Chinese cities. The reduction of CO and $SO_2$ with the population was found to be small. While CO is found to decrease significantly during the lockdown, the net decline is uniform being a regional pollutant with a longer lifetime. $O_3$ shows the enhancement with the population density due to the higher reduction $NO_x$ in the populated areas.

### 3.7. Spatial inter-correlation of pollutants during the lockdown

Spatial correlation analysis has been conducted to study the changes in the linear relations between the gaseous and particulate pollutants. Supplementary Figure S8 shows the scatter plot and spatial correlation of the average pollutant concentration observed at measurement locations during the lockdown in 2020 and 2017–2019. Particulate matter ($PM_{10}$ and $PM_{2.5}$) is positively correlated with $NO_2$, CO and $SO_2$ during the lockdown in 2020 as well as in 2017–2019. As these are emitted from primary emission sources, they are likely to have a positive correlation. Moreover, $SO_2$ and $NO_2$, the precursors of sulfate and nitrate aerosols, are likely to have positive correlations with PM when the composition of PM is dominated by secondary aerosols (Huang et al., 2012). As CO is not a

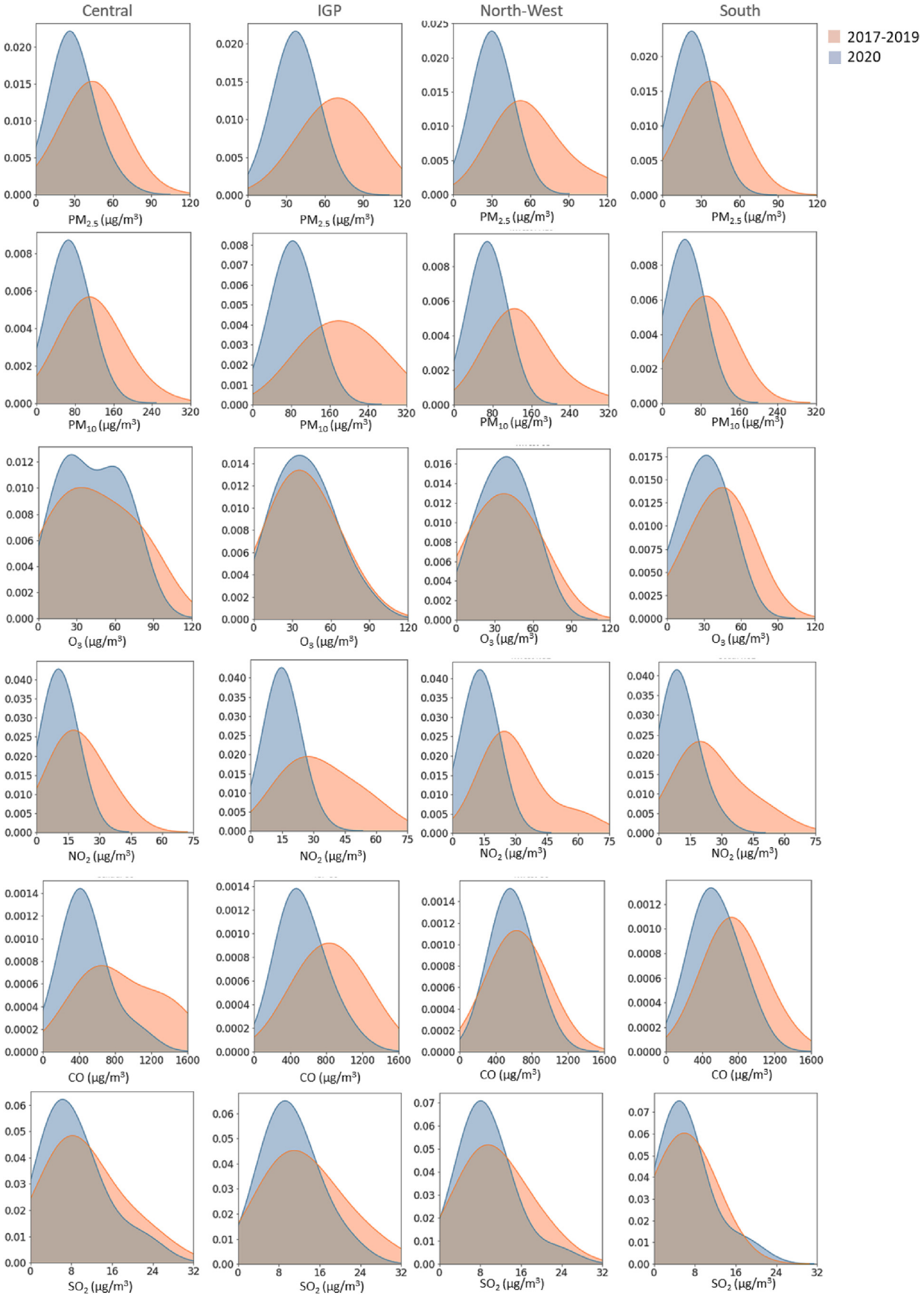


**Fig. 7.** Probability density function (PDF) of the pollutants during the lockdown in 2020 and during the same period in 2017–2019.

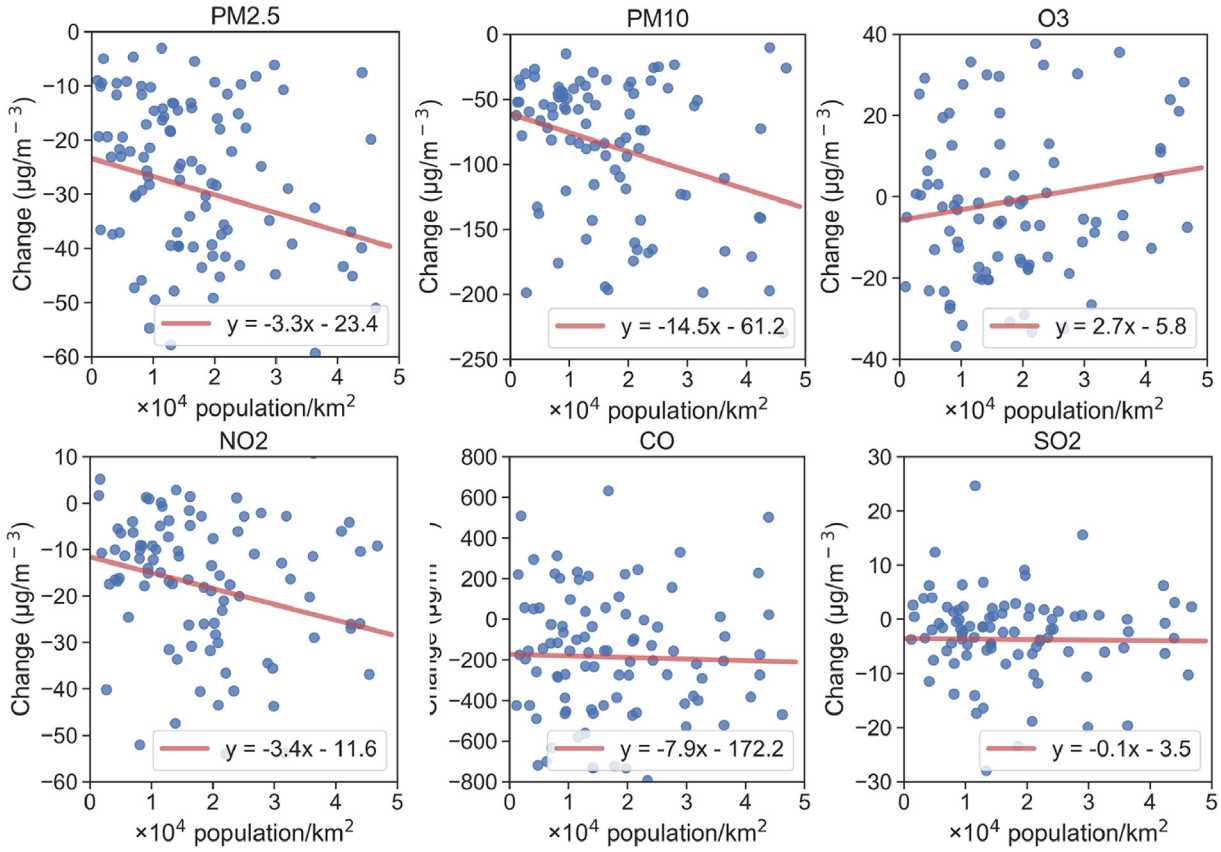


**Fig. 8.** Scatter plot of the change in the pollution during lockdown vs the population density at the location of the pollution monitoring.

precursor of secondary aerosol, the positive correlation between $NO_2$ and CO is because of the positive correlation of CO with PM.

$O_3$ exhibits no significant correlation with $PM_{10}$, $PM_{2.5}$, and $SO_2$; and negative correlation with $NO_2$ and CO in 2017–2019. The negative correlation suggests that $O_3$ levels were decreasing with the increase of $NO_2$ and CO. The urban areas in India are VOC limited (Sharma et al., 2016; Kumar et al., 2008), therefore lowering $NO_2$ levels will lead to an increase in $O_3$ owing to the reduction in the $O_3$ loss process (Seinfeld and Pandis, 2006) and exhibit a negative correlation. However, during the lockdown, $O_3$ is found to be positively correlated with $PM_{10}$, $PM_{2.5}$, $NO_2$ and $SO_2$. It is possible that the VOC/NOx ratio may have increased due to a significant reduction in anthropogenic NOx emissions. This makes the $O_3$ limited by NOx concentration where $O_3$ varies linearly with NOx. The positive correlation with $O_3$ with PM is due to the correlation of PM emissions with NOx emissions.

### 3.8. Air pollution changes in megacity Delhi

Several measures (MoEFCC, 2019) are in place to reduce the pollution in the National capital Delhi, which is one of the polluted megacities in the world (WHO, 2018: Gurjar et al., 2016; Ravindra et al., 2016). Owing to its geography, meteorology, direct and indirect emission sources, and burgeoning population, the city receives more number of air pollution events (Singh et al., 2020a; Hama et al., 2020; Beig et al., 2020; Ravindra et al., 2019a), which affects the social and economic health of the city. In the current scenario of nationwide lockdown, it is crucial to study the changes in air pollution in megacity Delhi. This analysis considers all the available stations in monitoring sites in Delhi having valid data.

The overall reduction in the six criteria pollutants estimated for Delhi has been shown in Fig. 9. The box and whisker plots shown in Fig. 9 describe the statistical details of reduction, including median,

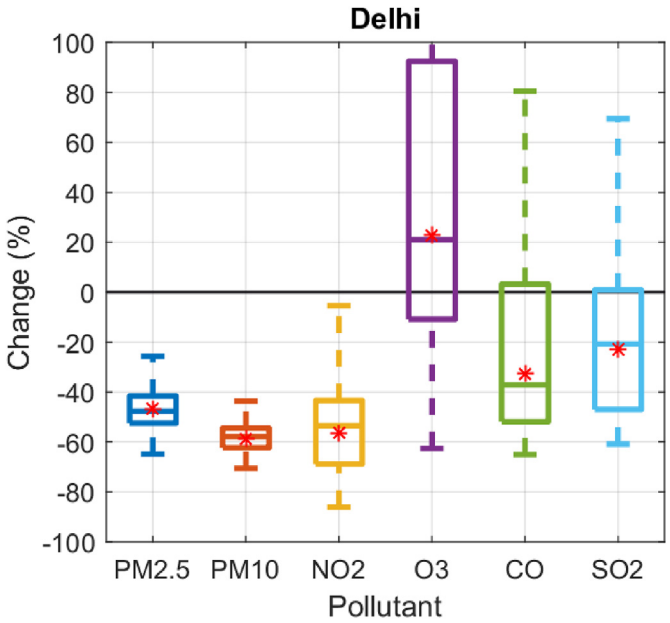


**Fig. 9.** Percentage change in the six criteria pollutants during the first two phases of lockdown in National Capital Delhi. The line in the box shows the median value, red star indicates the mean value. and the box shows the interquartile range. (For interpretation of the references to colour in this figure legend, the reader is referred to the Web version of this article.)

IQR (25$^{th}$ and 75$^{th}$ percentile) and the red star shows the average percentage change. As can be seen from the plot, the median percentage change shows a reduction for all the pollutants except $O_3$. The average highest reduction is observed for $PM_{10}$ (~59%), followed by $NO_2$ (56%), $PM_{2.5}$ (~47%), CO (~33%), $SO_2$ (~23%) whereas an increase of 23% is observed in $O_3$. The reduction in $PM_{10}$, $PM_{2.5}$ and $NO_2$ could be mainly attributed to restrictions imposed on vehicular movement. The larger reduction in $PM_{10}$ than $PM_{2.5}$ can be attributed to the reduced construction activities as well as to the dust re-suspension related to vehicular movement (Singh et al., 2020b), which were restricted during the lockdown. The temporary decrease in vehicular and industrial emission, fossil fuel combustion, and biomass burning led to a significant reduction in $PM_{2.5}$ levels. Our results for both the fractions of PM are consistent with the previously reported results by Mahato et al. (2020) for Delhi based on the data up to April 14, 2020.

Significant reduction in both the fractions of PM and NOx suggests that anthropogenic activities of Delhi and nearby regions define nearly half of the observed concentration levels during normal days (Gurjar et al., 2016). $O_3$ was observed to increase over Delhi at most of the sites because of the increased photochemical production of $O_3$ due to the reduction in PM (Xing et al., 2017) as well as precursor availability and chemistry at the monitoring locations. The reductions for the pollutants reported are in line with those reported by Mahato et al. (2020), Sarfaraz et al. (2020), Navinya et al. (2020) and Jain and Sharma (2020). However, in contrast to our observation as well as other studies that found an increase in $O_3$ levels in urban areas, Jain and Sharma (2020) have reported 14% decline in the same for Delhi. The differences in the results of these studies could be due to the different reporting periods as well as the method of reporting the changes.

### 3.9. Limitations of this study

While interpreting the results, it must be considered that most of the CAAQMS monitoring sites are located in urban areas, therefore this study mostly represents the changes at the urban locations than at the regional/rural background. The changes in air pollution reported in the current study are during the strict lockdown period and should not be considered due to the lockdown. The changes in the pollutants are combined effect of changes in the emissions, local meteorology, atmospheric dynamics, and chemistry. For example, the north-west, the IGP, and the central part of India have been influenced by more than the normal number of events of western disturbances (WDs, Dimri et al., 2015; IMD press release, 2020) causing the pollution levels to reduce further. Possibly, the impact of WDs can be seen before the lockdown, as well as during lockdown. Moreover, the effect of large-scale dynamics, non-linear chemistry needs to be investigated before coming to the conclusions. While we are confident that the particulate matter ($PM_{2.5}$ and $PM_{10}$), $NO_2$, and CO had decreased considerably across all locations, the actual percentage change requires detailed analysis.

## 4. Conclusions and discussion

The nationwide lockdown in several countries due to the COVID-19 (SARS-CoV-2) pandemic has resulted in improvements in air quality across the Globe. This study estimates the changes in the six criteria air pollutants ($PM_{2.5}$ and $PM_{10}$, $NO_2$, $O_3$, CO, and $SO_2$) during the lockdown across India. Hourly averaged concentrations measured at 134 sites from 15$^{th}$ February to 3$^{rd}$ May from 2017 to 2020 were analysed to study the impact of lockdown measures in terms of changes in the temporal evolution, changes in a diurnal pattern, and percentage reduction. The air pollution monitoring sites were grouped according to the geographical regions (north, IGP, north-west, north-east, central, and South) based on their pollution status, sources, and data availability to discuss the overall impact of the lockdown. The changes in the pollutants were estimated by comparing the concentrations during the strict lockdown (25$^{th}$ March to 3$^{rd}$ May 2020) with the same period in 2017–2019.

The most significant and prominent reduction was observed for both $PM_{2.5}$ and $PM_{10}$ across all regions in India. The highest median reduction in $PM_{2.5}$ and $PM_{10}$ has been estimated for north-west and IGP regions, where the levels during the lockdown have been reduced by ~50–60%. A decrease of ~40% was estimated in the southern regions for both $PM_{2.5}$ and $PM_{10}$, whereas the central region shows a decline of ~25% and ~40% in $PM_{2.5}$ and $PM_{10}$, respectively. The IGP is the most populated region in India. Moreover, the air quality over the IGP and north-west regions are also influenced by the dust storms leading the high surface dust load. The reduced industrial and construction activities, along with the reduced movement of vehicles leading to the reduction of the exhaust and non-exhaust emissions, mainly resuspended dust, may lead to a reduction of the PM levels. The role of secondary particles has not been quantified in this study.

$NO_2$ has been found to decrease across all regions with significant reduction (~40–70%) over north-west, IGP and south regions as well as at many sites in the central region. The major sources of $NO_2$ are the combustion of fuel such as vehicular emission and fossil fuel-based power plants that could be the leading cause of reduction of $NO_2$ except for the central region where increasing biomass burning might have neutralized the decrease in $NO_2$ that has happed due to the lockdown.

CO has declined in the four regions during the lockdown, with the highest reduction in the IGP region. The levels of CO in all the regions reached the same levels during the lockdown. The impact of lockdown has been studies on the diurnal variation of the pollutants. The diurnal variation in $PM_{2.5}$ and $PM_{10}$ during the lockdown shows a significant reduction throughout the day. However, variability remains the same, and they continue to have bio-modal distribution. The absolute reduction was found to be higher during the night as well during the peak traffic hours. Similar observations were also made for the $NO_2$ and CO, and the highest reduction was noted during the night.

$O_3$ continued to have similar diurnal variations; however, the reduction in $O_3$ is found during the sunlight hours. The decrease in $NO_2$ during night hours is observed to be more than the day-time. Night-time enhancement in $O_3$ of ~20–30% or even higher in the IGP and north-west regions due to the reduction in the removal of $O_3$ at night (Brown et al., 2006). Moreover, heterogeneous chemistry near the surface involving aerosols can also be responsible for the direct loss of $O_3$ (Jacob, 2000). $O_3$ was found to have mixed variation but a considerable decrease in the South region.

The PDF analysis also suggests a reduction in $PM_{2.5}$, $PM_{10}$, $NO_2$ and CO concentrations, marginal reduction in $SO_2$ and no significant change in the probability distribution of $O_3$. The most probable levels of $PM_{2.5}$, $PM_{10}$, $NO_2$, CO, $SO_2$ and $O_3$ during the lockdown were 20–40 $\mu g/m^3$, 50–80 $\mu g/m^3$, 8–15 $\mu g/m^3$, 400–600 $\mu g/m^3$, 4–10 $\mu g/m^3$ and 20–40 $\mu g/m^3$ respectively. The amount of reduction observed for $PM_{2.5}$, $PM_{10}$, $NO_2$ was found to reduce with respect to population suggesting a larger decline in populated areas. However, the change in $O_3$ is found to increase with the population.

Air quality in the megacity Delhi improved significantly during the lockdown. The levels of $NO_2$, $PM_{10}$, and $PM_{2.5}$ reduce significantly (~40–60%), whereas a moderate decrease was observed for CO and $SO_2$. The $O_3$ in Delhi follows a site-specific trend but shows a mean increase of ~20% due to increased photolysis production because of the reduction in particulate matter over Delhi as well as

precursor availability and chemistry at the monitoring locations.

To mitigate air pollution in India, it was planned to implement source and sector-specific measures as a part of NCAP, which focuses on reducing air pollution in India (MoEFCC, 2019). The other measures include the reduction of vehicular emissions implementation of new emissions standards, reduction in road dust resuspension and other fugitive emissions, controlling the biomass/waste burning, controlling the industrial pollution, construction, and demolition activities. These measures are similar to the restrictions imposed during the lockdown. The actual reduction in emission due to the lockdown can vary from place to place. However, the changes in the consumption of petroleum products (PPAC, 2020) in April 2020 with reference to the data in April 2019 suggests 50–60% reduction in road transport-related fuel, ~90% reduction in aviation fuel and ~40% reduction in industries and 70% reduction in construction activities. The consumption in LPG rose by 12%, suggesting an increase in household emissions. Assuming these reductions as COVID19 lockdown scenario, this study observes a substantial decrease of ~50% in the PM and $NO_2$ at all the sites across India. Although air pollution reduction during lockdown does give an insight into the betterment of air quality, such imposition is not economically and socially feasible in normal days. However, the results provided in this study give an idea of the maximum limit of air pollution reduction achievable through capping of major emission activities in urban regions.

Historically, out of the six air pollutants $PM_{10}$ and $PM_{2.5}$ often exceeded the national ambient air quality standards, which remained the biggest challenge for air quality scientists and policymakers. During the lockdown, $PM_{10}$ and $PM_{2.5}$ levels were found well below the national ambient air quality standards. However, it has to be noted that lockdown was imposed during the spring-summer season when the pollution levels might have already reduced by more than 50%. The question remains open whether a similar kind of reduction could be expected during peak pollution season in winter. The findings of the study will help to understand the impact the strict measures (i.e. COVID lockdown restriction) on the air quality over India and will be an aid to clean air programmes and air pollution modeling in terms of scenario analysis.

## Credit statement

**Vikas Singh:** Conceptualization, formal analysis, Investigation, writing original draft, review, and editing, **Shweta Singh:** Writing original draft, investigation, reviewing and editing, **Akash Biswal:** Visualization, Investigation, writing, reviewing and editing, **Amit Kesarkar**: Discussion, investigation, reviewing and editing, **Ravindra Khaiwal:** Investigation, discussion, reviewing, and editing. **Suman Mor:** Discussion, investigation, reviewing and editing

## Declaration of competing interest

The authors declare that they have no known competing financial interests or personal relationships that could have appeared to influence the work reported in this paper.

## Acknowledgment

The authors are thankful to Dr. A.K. Patra, Director, National Atmospheric Research Laboratory (NARL, Gadanki, India), for encouragement to conduct this research and provide the necessary support. SS and AB greatly acknowledge the Ministry of Earth Sciences (MoES, India) for research fellowship. We acknowledge and thank Central Pollution Control Board (CPCB, India), respective state pollution control boards, Ministry of Environment, Forest and Climate Change (MoEFCC, India) for making available air quality data in public. The authors gratefully acknowledge the MERRA-2 meteorological data by NASA's GMAO and NOAA Air Resources Laboratory (ARL, United States) for the provision of the HYSPLIT transport and dispersion model. The authors are grateful to all the seven reviewers who have helped to improvise the manuscript. The conclusions drawn in the paper are based on the interpretation of results and in no way reflect the viewpoint of the funding agencies.

## Appendix A. Supplementary data

Supplementary data to this article can be found online at https://doi.org/10.1016/j.envpol.2020.115368.

## References

Abdullah, et al., 2020. Air Quality Status during 2020 Malaysia Movement Control Order (MCO) Due to 2019 Novel Coronavirus (2019-nCoV) Pandemic.

Bao, R., Zhang, A., 2020. Does lockdown reduce air pollution? Evidence from 44 cities in Northern China. Sci. Total Environ. 731, 139052.

Bashir, M.F., Ma, B.J., Bilal Komal, B., Bashir, M.A., Farooq, T.H., Iqbal, N., Bashir, M., 2020. Correlation between environmental pollution indicators and COVID-19 pandemic: a brief study in Californian context. Environ. Res. 187, 109652. https://doi.org/10.1016/j.envres.2020.109652.

Beig, G., Sahu, S.K., Singh, V., Tikle, S., Sobhana, S.B., Gargeva, P., et al., 2020. Objective evaluation of stubble emission of North India and quantifying its impact on air quality of Delhi. Sci. Total Environ. 709, 136126.

Brown, S.S., Ryerson, T.B., Wollny, A.G., Brock, C.A., Peltier, R., Sullivan, A.P., Weber, R.J., Dubé, W.P., Trainer, M., Meagher, J.F., Fehsenfeld, F.C., Ravishankara, A.R., 2006. Variability in nocturnal nitrogen oxide processing and its role in regional air quality. Science 311, 67–70. https://doi.org/10.1126/science.1120120.

Buchard, V., Randles, C.A., Da Silva, A.M., Darmenov, A., Colarco, P.R., Govindaraju, R., et al., 2017. The MERRA-2 aerosol reanalysis, 1980 onward. Part II: evaluation and case studies. J. Clim. 30 (17), 6851–6872.

Chauhan, A., Singh, R.P., 2020. Decline in PM2.5 concentrations over major cities around the world associated with COVID-19. Environ. Res. 109634. https://doi.org/10.1016/j.envres.2020.109634.

Chen, K., Wang, M., Huang, C., Kinney, P.L., Anastas, P.T., 2020. Air pollution reduction and mortality benefit during the COVID-19 outbreak in China. The Lancet Planetary Health.

Cheng, N., Zhang, D., Li, Y., Xie, X., Chen, Z., Meng, F., Gao, B., He, B., 2017. Spatio-temporal variations of PM 2.5 concentrations and the evaluation of emission reduction measures during two red air pollution alerts in Beijing. Sci. Rep. 7, 8220. https://doi.org/10.1038/s41598-017-08895-x.

Chowdhury, S., Dey, S., Tripathi, S.N., Beig, G., Mishra, A.K., Sharma, S., 2017. "Traffic intervention" policy fails to mitigate air pollution in megacity Delhi. Environ. Sci. Pol. 74, 8–13. https://doi.org/10.1016/j.envsci.2017.04.018.

Collivignarelli, M.C., Abbà, A., Bertanza, G., Pedrazzani, R., Ricciardi, P., Miino, M.C., 2020. Lockdown for CoViD-2019 in Milan: what are the effects on air quality? Sci. Total Environ. 732, 139280.

CPCB, 2009. National Ambient Air Quality Standards, Central Pollution Control Board Notification, New Delhi, 18th November, 2009 No.B-29016/20/90/PCI-. Accessed 03-Apr-2020. https://tspcb.cgg.gov.in/Environment/Ambient%20Air%20Quality_Standards_2009.pdf.

CPCB, 2019. Technical Specifications for Continuous Ambient Air Quality Monitoring (CAAQM) Station (Real Time). https://cpcb.nic.in/report.php.

Dantas, G., Siciliano, B., França, B.B., da Silva, C.M., Arbilla, G., 2020. The impact of COVID-19 partial lockdown on the air quality of the city of Rio de Janeiro, Brazil, vol. 729. Science of The Total Environment, p. 139085.

Dimri, A.P., Niyogi, D., Barros, A.P., Ridley, J., Mohanty, U.C., Yasunari, T., Sikka, D.R., 2015. Western disturbances: a review. Rev. Geophys. 53, 225–246. https://doi.org/10.1002/2014RG000460.

Dutheil, F., Baker, J.S., Navel, V., 2020. COVID-19 as a factor influencing air pollution? Environ. Pollut. https://doi.org/10.1016/j.envpol.2020.114466.

ESA, 2020. Air Pollution Drops in India Following Lockdown. https://www.esa.int/Applications/Observing_the_Earth/Copernicus/Sentinel-5P/Air_pollution_drops_in_India_following_lockdown.

Eskridge, R.E., Ku, J.Y., Rao, S.T., Porter, P.S., Zurbenko, I.G., 1997. Separating different scales of motion in time series of meteorological variables. Bull. Am. Meteorol. Soc. 78 (7), 1473–1484.

Fan, C., Li, Y., Guang, J., Li, Z., Elnashar, A., Allam, M., de Leeuw, G., 2020. The impact of the control measures during the COVID-19 outbreak on air pollution in China. Rem. Sens. 12 (10), 1613.

Fattorini, D., Regoli, F., 2020. Role of the Chronic Air Pollution Levels in the Covid-19 Outbreak Risk in Italy. Environmental Pollution, p. 114732.

Filippini, T., Rothman, K.J., Goffi, A., Ferrari, F., Maffeis, G., Orsini, N., Vinceti, M., 2020. Satellite-detected Tropospheric Nitrogen Dioxide and Spread of SARS-CoV-2 Infection in Northern Italy. Science of The Total Environment, p. 140278.

Forouzanfar, Mohammad H., Afshin, Ashkan, Lily, T., Alexander, H., Anderson, Ross,

Bhutta, Zulfiqar A., Biryukov, Stan, Brauer, Michael, et al., 2016. "Global, regional, and national comparative risk assessment of 79 behavioural, environmental and occupational, and metabolic risks or clusters of risks, 1990–2015: a systematic analysis for the global burden of disease study 2015. Lancet 388 (October 8), 1659–1724. https://doi.org/10.1016/S0140-6736(16)31679-8, 10053.

Gaur, A., Tripathi, S.N., Kanawade, V.P., Tare, V., Shukla, S.P., 2014. Four-year measurements of trace gases (SO2, NOx, CO, and O3) at an urban location, Kanpur, in Northern India. J. Atmos. Chem. 71, 283–301. https://doi.org/10.1007/s10874-014-9295-8.

Gelaro, R., McCarty, W., Suárez, M.J., Todling, R., Molod, A., Takacs, L., et al., 2017. The modern-era retrospective analysis for research and applications, version 2 (MERRA-2). J. Clim. 30 (14), 5419–5454.

Ghosh, D., Lal, S., Sarkar, U., 2017. Variability of tropospheric columnar NO 2 and SO 2 over eastern Indo-Gangetic Plain and impact of meteorology. Air Quality, Atmosphere & Health 10 (5), 565–574.

GLA, 2020. Estimation of Changes in Air Pollution in London during the COVID19 Outbreak. https://www.london.gov.uk/sites/default/files/london_response_to_aqeg_call_for_evidence_april_2020.pdf.

Gurjar, B.R., Ravindra, K., Nagpure, A.S., 2016. Air pollution trends over Indian megacities and their local-to-global implications. Atmos. Environ. 142, 475–495.

Guttikunda, S.K., Nishadh, K.A., Jawahar, P., 2019. Air pollution knowledge assessments (APnA) for 20 Indian cities. Urban Climate 27, 124–141. https://doi.org/10.1016/j.uclim.2018.11.005.

Hama, S.M.L., Kumar, P., Harrison, R.M., Bloss, W.J., Khare, M., Mishra, S., Namdeo, A., Sokhi, R., Goodman, P., Sharma, C., 2020. Four-year assessment of ambient particulate matter and trace gases in the Delhi-NCR region of India. Sustainable Cities and Society 54, 102003. https://doi.org/10.1016/j.scs.2019.102003.

Hogrefe, C., Vempaty, S., Rao, S.T., Porter, P.S., 2003. A comparison of four techniques for separating different time scales in atmospheric variables. Atmos. Environ. 37, 313–325. https://doi.org/10.1016/S1352-2310(02)00897-X.

Holloway, T., Levy, H., Kasibhatla, P., 2000. Global distribution of carbon monoxide. J. Geophys. Res.: Atmosphere 105 (D10), 12123–12147.

Huang, K., Zhuang, G., Lin, Y., Fu, J.S., Wang, Q., Liu, T., Zhang, R., Jiang, Y., Deng, C., Fu, Q., Hsu, N.C., Cao, B., 2012. Typical types and formation mechanisms of haze in an Eastern Asia megacity, Shanghai, Atmos. Chem. Phys. 12, 105–124. https://doi.org/10.5194/acp-12-105-2012.

Huang, X., Ding, A., Gao, J., Zheng, B., Zhou, D., Qi, X., et al., 2020. Enhanced Secondary Pollution Offset Reduction of Primary Emissions during COVID-19 Lockdown in China.

Im, U., Bianconi, R., Solazzo, E., Kioutsioukis, I., Badia, A., Balzarini, A., Baró, R., Bellasio, R., Brunner, D., Chemel, C., Curci, G., 2015a. Evaluation of operational on-line-coupled regional air quality models over Europe and North America in the context of AQMEII phase 2. Part I: Ozone, 115. Atmospheric environment, pp. 404–420.

Im, U., Bianconi, R., Solazzo, E., Kioutsioukis, I., Badia, A., Balzarini, A., Baró, R., Bellasio, R., Brunner, D., Chemel, C., Curci, G., 2015b. Evaluation of Operational Online-Coupled Regional Air Quality Models over Europe and North America in the Context of AQMEII Phase 2. Part II: Particulate Matter, vol. 115. Atmospheric Environment, pp. 421–441.

IMD Press Release, 2020. https://mausam.imd.gov.in/imd_latest/contents/press_release.php. https://mausam.imd.gov.in/backend/assets/press_release_pdf/PWB_22-03-2020.pdf.

Isaifan, R.J., 2020. The dramatic impact of Coronavirus outbreak on air quality: has it saved as much as it has killed so far? Global Journal of Environmental Science and Management 6 (3), 275–288.

Jacob, D.J., 2000. Heterogeneous chemistry and tropospheric ozone. Atmos. Environ. 34, 2131–2159. https://doi.org/10.1016/S1352-2310(99)00462-8.

Jain, S., Sharma, T., 2020. Social and travel lockdown impact considering coronavirus disease (COVID-19) on air quality in megacities of India: present benefits, future challenges and way forward. Aerosol and Air Quality Research 20, 1222–1236.

Kanniah, K.D., Zaman, N.A.F.K., Kaskaoutis, D.G., Latif, M.T., 2020. COVID-19's Impact on the Atmospheric Environment in the Southeast Asia Region. Science of The Total Environment, p. 139658.

Kaur-Sidhu, M., Ravindra, K., Mor, S., John, S., 2020. Emission factors and global warming potential of various solid biomass fuel-cook stove combinations. Atmospheric Pollution Research 11 (2), 252–260.

Kerimray, A., Baimatova, N., Ibragimova, O.P., Bukenov, B., Kenessov, B., Plotitsyn, P., Karaca, F., 2020. Assessing Air Quality Changes in Large Cities during COVID-19 Lockdowns: the Impacts of Traffic-free Urban Conditions in Almaty. Science of the Total Environment, Kazakhstan, 139179.

Krecl, P., Targino, A.C., Oukawa, G.Y.C., Junior, R.P.C., 2020. Drop in Urban Air Pollution from COVID-19 Pandemic: Policy Implications for the Megacity of São Paulo. Environmental Pollution (Barking, Essex: 1987).

Kumar, M., Parmar, K.S., Kumar, D.B., Mhawish, A., Broday, D.M., Mall, R.K., Banerjee, T., 2018. Long-term aerosol climatology over Indo-Gangetic Plain: trend, prediction and potential source fields. Atmos. Environ. 180, 37–50.

Kumar, R., Naja, M., Pfister, G.G., Barth, M.C., Wiedinmyer, C., Brasseur, G.P., 2012. Simulations over south asia using the weather research and forecasting model with chemistry (WRF-Chem): chemistry evaluation and initial results. Geosci. Model Dev. (GMD) 5, 619–648. https://doi.org/10.5194/gmd-5-619-2012.

Kumar, U., Prakash, A., Jain, V.K., 2008. A photochemical modelling approach to investigate O3 sensitivity to NOx and VOCs in the urban atmosphere of Delhi. Aerosol Air Qual. Res. 8, 147–159. https://doi.org/10.4209/aaqr.2007.09.0037.

Kumari, P., Toshniwal, D., 2020. Impact of lockdown measures during COVID-19 on air quality–A case study of India. Int. J. Environ. Health Res. 1–8.

Lal, P., Kumar, A., Kumar, S., Kumari, S., Saikia, P., Dayanandan, A., et al., 2020. The Dark Cloud with a Silver Lining: Assessing the Impact of the SARS COVID-19 Pandemic on the Global Environment. Science of The Total Environment, 139297.

Lal, S., Naja, M., Subbaraya, B.H., 2000. Seasonal variations in surface ozone and its precursors over an urban site in India. Atmos. Environ. 34, 2713–2724. https://doi.org/10.1016/S1352-2310(99)00510-5.

Li, L., Li, Q., Huang, L., Wang, Q., Zhu, A., Xu, J., Liu, Z., Li, H., Shi, L., Li, R., Azari, M., 2020. Air Quality Changes during the COVID-19 Lockdown over the Yangtze River Delta Region: an Insight into the Impact of Human Activity Pattern Changes on Air Pollution Variation. Science of The Total Environment, p. 139282.

Li, L., Chen, Z.M., Zhang, Y.H., Zhu, T., Li, S., Li, H.J., Zhu, L.H., Xu, B.Y., 2007. Heterogeneous oxidation of sulfur dioxide by ozone on the surface of sodium chloride and its mixtures with other components. J. Geophys. Res.: Atmosphere 112. https://doi.org/10.1029/2006JD008207.

Li, L., Zhu, S., An, J., Zhou, M., Wang, H., Yan, R., Qiao, L., Tian, X., Shen, L., Huang, L., Wang, Y., Huang, C., Avise, J.C., Fu, J.S., 2019. Evaluation of the effect of regional joint-control measures on changing photochemical transformation: a comprehensive study of the optimization scenario analysis. Atmos. Chem. Phys. 19, 9037–9060. https://doi.org/10.5194/acp-19-9037-2019.

Lu, X., Zhang, L., Liu, X., Gao, M., Zhao, Y., Shao, J., 2018. Lower tropospheric ozone over India and its linkage to the South Asian monsoon. Atmos. Chem. Phys. 18, 3101–3118. https://doi.org/10.5194/acp-18-3101-2018.

Lu, Z., Streets, D.G., de Foy, B., Krotkov, N.A., 2013. Ozone Monitoring Instrument observations of interannual increases in SO2 emissions from Indian coal-fired power plants during 2005–2012. Environ. Sci. Technol. 47 (24), 13993–14000.

Mahato, S., Pal, S., Ghosh, K.G., 2020. Effect of Lockdown amid COVID-19 Pandemic on Air Quality of the Megacity Delhi, India. Science of The Total Environment, p. 139086.

Mallik, C., Lal, S., 2014. Seasonal characteristics of SO2, NO2, and CO emissions in and around the Indo-Gangetic Plain. Environ. Monit. Assess. 186, 1295–1310. https://doi.org/10.1007/s10661-013-3458-y.

Mandal, I., Pal, S., 2020. COVID-19 Pandemic Persuaded Lockdown Effects on Environment over Stone Quarrying and Crushing Areas. Science of The Total Environment, 139281.

Masiol, M., Squizzato, S., Formenton, G., Harrison, R.M., Agostinelli, C., 2017. Air Quality across a European Hotspot: Spatial Gradients, Seasonality, Diurnal Cycles and Trends in the Veneto Region, NE Italy, vol. 576. Science of The Total Environment, pp. 210–224.

Menut, L., Bessagnet, B., Siour, G., Mailler, S., Pennel, R., Cholakian, A., 2020. Impact of Lockdown Measures to Combat Covid-19 on Air Quality over Western Europe. Science of The Total Environment, p. 140426.

MHA, 2020. No.40-3/2020-DM-I (A), Government of India. Ministry of Home Affairs. https://www.mha.gov.in/sites/default/files/MHA%20order%20dt%2015.04.2020%2C%20with%20Revised%20Consolidated%20Guidelines_compressed%20%283%29.pdf. http://www.du.ac.in/du/uploads/PR_Consolidated%20Guideline%20of%20MHA_28032020%20(1)_1.PDF.

Muhammad, S., Long, X., Salman, M., 2020. COVID-19 Pandemic and Environmental Pollution: A Blessing in Disguise? Science of The Total Environment, p. 138820.

Nakada, L.Y.K., Urban, R.C., 2020. COVID-19 Pandemic: Impacts on the Air Quality during the Partial Lockdown in São Paulo State, Brazil. Science of The Total Environment, p. 139087.

Navinya, C., Patidar, G., Phuleria, H.C., 2020. Examining effects of the COVID-19 national lockdown on ambient air quality across urban India. Aerosol Air Qual. Res. https://doi.org/10.4209/aaqr.2020.05.0256.

NCAP, MoEFCC, Ministry of Environment, 2019. Forest and Climate Change. MoEFCC, Ministry of Environment, Forest & Climate Change NCAP- National Clean Air Programme (2019), pp. 1–106. http://moef.gov.in/wp-content/uploads/2019/05/NCAP_Report.pdf.

Otmani, A., Benchrif, A., Tahri, M., Bounakhla, M., El Bouch, M., Krombi, M.H., 2020. Impact of Covid-19 Lockdown on PM10, SO2 and NO2 Concentrations in Salé City (Morocco). Science of The Total Environment, p. 139541.

Pant, P., Lal, R.M., Guttikunda, S.K., Russell, A.G., Nagpure, A.S., Ramaswami, A., Peltier, R.E., 2019. Monitoring particulate matter in India: recent trends and future outlook. Air Quality, Atmosphere & Health 12 (1), 45–58.

Parajuli, S.P., Zender, C.S., 2017. Connecting geomorphology to dust emission through high-resolution mapping of global land cover and sediment supply. Aeolian Research 27, 47–65. https://doi.org/10.1016/j.aeolia.2017.06.002.

PPAC, 2020. Consumption of Petroleum Products, Petroleum Planning & Analysis Cell. https://www.ppac.gov.in/content/147_1_ConsumptionPetroleum.aspx.

Purohit, P., Amann, M., Kiesewetter, G., Rafaj, P., Chaturvedi, V., Dholakia, H.H., Koti, P.N., Klimont, Z., Borken-Kleefeld, J., Gomez-Sanabria, A., Schöpp, W., Sander, R., 2019. Mitigation pathways towards national ambient air quality standards in India. Environ. Int. 133, 105147. https://doi.org/10.1016/j.envint.2019.105147.

Randles, C.A., Da Silva, A.M., Buchard, V., Colarco, P.R., Darmenov, A., Govindaraju, R., et al., 2017. The MERRA-2 aerosol reanalysis, 1980 onward. Part I: system description and data assimilation evaluation. J. Clim. 30 (17), 6823–6850.

Ravindra, K., Kaur-Sidhu, M., Mor, S., John, S., 2019c. Trend in household energy consumption pattern in India: a case study on the influence of socio-cultural factors for the choice of clean fuel use. J. Clean. Prod. 213, 1024–1034.

Ravindra, K., Sidhu, M.K., Mor, S., John, S., Pyne, S., 2016. Air pollution in India: bridging the gap between science and policy. Journal of Hazardous, Toxic, and Radioactive Waste 20 (4), A4015003.
Ravindra, K., Singh, T., Mor, S., 2019b. Emissions of air pollutants from primary crop residue burning in India and their mitigation strategies for cleaner emissions. J. Clean. Prod. 208, 261–273.
Ravindra, K., Singh, T., Mor, S., Singh, V., Mandal, T.K., Bhatti, M.S., Gahlawat, S.K., Dhankhar, R., Mor, S., Beig, G., 2019a. Real-time monitoring of air pollutants in seven cities of North India during crop residue burning and their relationship with meteorology and transboundary movement of air. Sci. Total Environ. 690, 717–729.
Ravindra, K., Singh, T., Pandey, V., Mor, S., 2020. Air Pollution Trend in Chandigarh City Situated in Indo-Gangetic Plains: Understanding Seasonality and Impact of Mitigation Strategies. Science of The Total Environment, p. 138717.
Reddy, B.S.K., Kumar, K.R., Balakrishnaiah, G., Gopal, K.R., Reddy, R.R., Sivakumar, V., et al., 2012. Analysis of diurnal and seasonal behavior of surface ozone and its precursors (NOx) at a semi-arid rural site in southern India. Aerosol Air Qual Res 12, 1081–1094.
Sahu, L.K., Sheel, V., Pandey, K., Yadav, R., Saxena, P., Gunthe, S., 2015. Regional biomass burning trends in India: analysis of satellite fire data. J Earth Syst Sci 124, 1377–1387. https://doi.org/10.1007/s12040-015-0616-3.
Sarfraz, M., Shehzad, K., Meran Shah, S.G., 2020. The impact of COVID-19 as a necessary evil on air pollution in India during the lockdown. Environ. Pollut. 115080 https://doi.org/10.1016/j.envpol.2020.115080.
Schnell, J.L., Naik, V., Horowitz, L.W., Paulot, F., Mao, J., Ginoux, P., Zhao, M., Ram, K., 2018. Exploring the relationship between surface PM2.5 and meteorology in Northern India. Atmos. Chem. Phys. 18, 10157–10175. https://doi.org/10.5194/acp-18-10157-2018.
Seinfeld, J.H., Pandis, S.N., 2006. Atmospheric Chemistry and Physics. A Wiley-Inter Science Publication. John Wiley & Sons Inc, New York.
Selvam, S., Muthukumar, P., Venkatramanan, S., Roy, P.D., Bharath, K.M., Jesuraja, K., 2020. SARS-CoV-2 pandemic lockdown: effects on air quality in the industrialized Gujarat state of India. Science of The Total Environment, p. 140391.
Seo, J., Park, D.-S.R., Kim, J.Y., Youn, D., Lim, Y.B., Kim, Y., 2018. Effects of meteorology and emissions on urban air quality: a quantitative statistical approach to long-term records (1999–2016) in Seoul, South Korea. Atmos. Chem. Phys. 18, 16121–16137. https://doi.org/10.5194/acp-18-16121-2018.
Sharma, M., Dikshit, O., 2016. Comprehensive Study on Air Pollution and Green House Gases (GHGs) in Delhi. A report submitted to Government of NCT Delhi and DPCC Delhi, pp. 1–334.
Sharma, S., Chatani, S., Mahtta, R., Goel, A., Kumar, A., 2016. Sensitivity analysis of ground level ozone in India using WRF-CMAQ models. Atmos. Environ. 131, 29–40.
Sharma, S., Zhang, M., Gao, J., Zhang, H., Kota, S.H., 2020. Effect of restricted emissions during COVID-19 on air quality in India. Sci. Total Environ. 728, 138878.
Sicard, P., De Marco, A., Agathokleous, E., Feng, Z., Xu, X., Paoletti, E., Rodriguez, J.J.D., Calatayud, V., 2020. Amplified Ozone Pollution in Cities during the COVID-19 Lockdown. Science of The Total Environment, p. 139542.
Singh, V., Biswal, A., Kesarkar, A.P., Mor, S., Ravindra, K., 2020a. High resolution vehicular PM10 emissions over megacity Delhi: relative contributions of exhaust and non-exhaust sources. Sci. Total Environ. 699, 134273. https://doi.org/10.1016/j.scitotenv.2019.134273.
Singh, V., Ravindra, K., Sahu, L., Sokhi, R., 2018a. Trends of Atmospheric Black Carbon Concentration over the United Kingdom, vol. 178. Atmospheric environment, pp. 148–157.
Singh, V., Sahu, S.K., Kesarkar, A.P., Biswal, A., 2018b. Estimation of high resolution emissions from road transport sector in a megacity Delhi. Urban Climate 26, 109–120. https://doi.org/10.1016/j.uclim.2018.08.011.
Singh, V., Singh, S., Biswal, A., 2020b. Exceedances and trends of particulate matter ($PM_{2.5}$) in five Indian megacities. Science of the Total Environment. https://doi.org/10.1016/j.scitotenv.2020.141461. In press.
Srivastava, S., Kumar, A., Bauddh, K., Gautam, A.S., Kumar, S., 2020. 21-Day lockdown in India dramatically reduced air pollution indices in Lucknow and New Delhi, India. Bull. Environ. Contam. Toxicol. 1.
Stein, A.F., Draxler, R.R., Rolph, G.D., Stunder, B.J.B., Cohen, M.D., Ngan, F., 2015. NOAA's HYSPLIT atmospheric transport and dispersion modeling system. Bull. Am. Meteorol. Soc. 96, 2059–2077. https://doi.org/10.1175/BAMS-D-14-00110.1.
Tang, Y.S., Braban, C.F., Dragosits, U., Dore, A.J., Simmons, I., van Dijk, N., Poskitt, J., Dos Santos Pereira, G., Keenan, P.O., Conolly, C., Vincent, K., 2018. Drivers for spatial, temporal and long-term trends in atmospheric ammonia and ammonium in the UK. Atmos. Chem. Phys. 18 (2), 705–733.
Tobías, A., Carnerero, C., Reche, C., Massagué, J., Via, M., Minguillón, M.C., Alastuey, A., Querol, X., 2020. Changes in air quality during the lockdown in Barcelona (Spain) one month into the SARS-CoV-2 epidemic. Science of The Total Environment, p. 138540.
Venkataraman, C., Habib, G., Kadamba, D., Shrivastava, M., Leon, J.-F., Crouzille, B., Boucher, O., Streets, D.G., 2006. Emissions from open biomass burning in India: integrating the inventory approach with high-resolution Moderate Resolution Imaging Spectroradiometer (MODIS) active-fire and land cover data. Global Biogeochem. Cycles 20, GB2013. https://doi.org/10.1029/2005GB002547.
Wang, P., Chen, K., Zhu, S., Wang, P., Zhang, H., 2020b. Severe air pollution events not avoided by reduced anthropogenic activities during COVID-19 outbreak. Resour. Conserv. Recycl. 158, 104814.
Wang, Y., Yuan, Y., Wang, Q., Liu, C., Zhi, Q., Cao, J., 2020a. Changes in Air Quality Related to the Control of Coronavirus in China: Implications for Traffic and Industrial Emissions. Science of The Total Environment, p. 139133.
WHO, 2018. WHO Global Ambient Air Quality Database (Update 2018). https://www.who.int/airpollution/data/cities/en/.
WorldPop, 2017. India 100m Population. University of Southampton. https://doi.org/10.5258/SOTON/WP00532. Version 2.
Xing, J., Mathur, R., Pleim, J., Hogrefe, C., Gan, C.M., Wong, D.C., Wei, C., Gilliam, R., Pouliot, G., 2015. Observations and modeling of air quality trends over 1990–2010 across the Northern Hemisphere: China, the United States and Europe. Atmos. Chem. Phys. 15 (5), 2723–2747.
Xing, J., Wang, J., Mathur, R., Wang, S., Sarwar, G., Pleim, J., Hogrefe, C., Zhang, Y., Jiang, J., Wong, D.C., Hao, J., 2017. Impacts of aerosol direct effects on tropospheric ozone through changes in atmospheric dynamics and photolysis rates. Atmos. Chem. Phys. 17, 9869–9883. https://doi.org/10.5194/acp-17-9869-2017.
Yadav, R., Sahu, L.K., Beig, G., Tripathi, N., Jaaffrey, S.N.A., 2017. Ambient particulate matter and carbon monoxide at an urban site of India: influence of anthropogenic emissions and dust storms. Environ. Pollut. 225, 291–303.
Yin, S., Wang, X., Zhang, X., Guo, M., Miura, M., Xiao, Y., 2019. Influence of biomass burning on local air pollution in mainland Southeast Asia from 2001 to 2016. Environ. Pollut. 254, 112949.
Yongjian, Z., Jingu, X., Fengming, H., Liqing, C., 2020. Association between Short-Term Exposure to Air Pollution and COVID-19 Infection: Evidence from China. Science of the total environment, p. 138704.
Zambrano-Monserrate, M.A., Ruano, M.A., Sanchez-Alcalde, L., 2020. Indirect effects of COVID-19 on the environment. Science of the Total Environment 728. https://doi.org/10.1016/j.scitotenv.2020.138813.
Zheng, H., Kong, S., Chen, N., Yan, Y., Liu, D., Zhu, B., et al., 2020. Significant Changes in the Chemical Compositions and Sources of PM2. 5 in Wuhan since the City Lockdown as COVID-19. Science of The Total Environment, p. 140000.